UNIVERSITEIT VAN PRETORIA
UNIVERSITY OF PRETORIA
YUNIBESITHI YA PRETORIA

Development of fluorescence-based assays to determine changes in membrane potential and K^+ levels in isolated *Plasmodium falciparum* parasites

Jean Argyle Thomas

(u17075395)

Submitted in fulfilment of the requirements for the degree

Magister Scientiae in Biochemistry

in the Faculty of Natural and Agricultural Sciences

Department of Biochemistry, Genetics and Microbiology Division of Biochemistry

University of Pretoria

4 March 2024

UNIVERSITEIT VAN PRETORIA
UNIVERSITY OF PRETORIA
YUNIBESITHI YA PRETORIA

Submission Declaration

I, Jean Argyle Thomas, declare that the dissertation, which I hereby submit for the degree *Magister Scientiae* in the Department of Biochemistry, Genetics and Microbiology at the University of Pretoria, is my own work and has not previously been submitted by me for a degree at this or any other tertiary institution.

Signature: 

Date: 04-03-2024

Declaration of originality

University of Pretoria

Faculty of Natural and Agricultural Sciences

Department of Biochemistry, Genetics and Microbiology

Full name of student: Jean Argyle Thomas

Student number: 17075395

Declaration

1. I understand what plagiarism is and am aware of the University's policy in this regard.
2. I declare that this dissertation is my own original work. Where other people's work has been used (either from a printed source, Internet or any other source), this has been properly acknowledged and referenced in accordance with Departmental requirements.
3. I have not used work previously produced by another student or any other person to hand in as my own.
4. I have not allowed, and will not allow, anyone to copy my work with the intention of passing it off as his or her own work.

Signature: 

Date: 04-03-2024

Table of Contents

List of Figures

List of Tables

List of Abbreviations

APG	Assante Potassium Green
BK	Big conductance Ca^{2+}-activated K^+ channel
CV	Coefficient of variation
$DiBAC_4(3)$	Bis(1,3-Dibutylbarbituric Acid) Trimethine Oxonol
EDC	Exoerythrocytic developmental cycle
EPM	Erythrocyte plasma membrane
hERG	Ether-à-go-go related gene
hpi	Hours post-invasion
HPLC	High performance liquid chromatography
IC_{50}	Half-maximal inhibitory concentration
IDC	Intraerythrocytic developmental cycle
IK	Intermediate conductance K^+ channel
IPTp	Intermittent preventive treatment of malaria in pregnancy
IRS	Indoor residual spraying
IVIEWGA	*In vitro* evolution and whole-genome analysis
Kv	Voltage-gated potassium channel
LLINs	Long-lasting insecticidal nets
MoA	Mode of action
NPPs	New permeation pathways
PBFI	Potassium binding benzofuran isopthalate
PfATP4	*Plasmodium falciparum* P-type ATP4
PVM	Parasitophorous vacuolar membrane
PPM	Parasite plasma membrane
PSAC	*Plasmodium* surface anion channel
S/B	Signal-to-background
SBFI	Sodium binding benzofuran isopthalate
S.E.	Standard error of the mean
SP	Sulfadoxine-pyrimethamine
TAPs	Triaminopyrimidines
V-type ATPase	Vacuolar-type H^+-ATPase
$\Delta\psi$	Membrane potential

Acknowledgements

Firstly, I would like to thank God for giving me the strength and determination throughout this project.

Secondly, I would like to express my appreciation to my supervisor, Dr. Jandeli Niemand, with whom out this would not have been possible. I would like to thank her for her patience and guidance throughout this degree as well as the skills and knowledge she shared with me. I also thank my co-supervisor Professor Lyn-Marie Birkholtz for her contribution. I would like to extend my appreciation to the Malaria Parasite Molecular Laboratory (M2PL) team who was always willing to help when needed.

Additionally, I thank my parents (Arra and Lyndi Thomas) for their endless support and encouragement they give me and without them this would not have been possible. I also thank my friends for listening to me and giving me advice when needed. I am also thankful for my lab partners who over this time have become friends including Shante da Rocha, Sizwe Tshabalala, Marche Mare, Henrico Langevled, Martha Muruya, Dana Schultz, Daniel Opperman and Savannah Watson. I thank them for their friendship, support, advice and for helping me without hesitation when things seemed impossible.

Lastly, I acknowledge the National Research Foundation for funding this degree.

Summary

While malaria is a treatable disease caused by *Plasmodium* parasites, resulting in worldwide mortality. *Plasmodium falciparum* parasites are vulnerable to changes in intracellular ion concentrations. The parasite Na^+/H^+-ATPase (PfATP4) responsible for the simultaneous efflux of Na^+ and the influx of H^+ is targeted by chemically diverse antiplasmodial compounds, while triaminopyrimidine resistance is associated with mutations in a V-type H^+-ATPase. In *P. falciparum* parasites, a high intracellular K^+ concentration is maintained by the influx of K^+ through K^+ channels, against the concentration gradient due to a highly negative membrane potential. Given that K^+ is the most abundant intracellular cation, it is possible that changing intracellular K^+ levels would prevent parasite proliferation. Any changes in the intracellular K^+ also affect the membrane potential, ultimately leading to cell death. Previous whole-cell proliferation assays showed that putative K^+ channel inhibitors and ionophores inhibit proliferation, but these studies did not test the antiproliferative effects with changes in intracellular K^+.

Intracellular K^+ can be measured using ion-selective electrodes, X-ray microanalysis, HPLC, flame photometry and atomic absorption. However, these techniques require complex sample preparation and often specialized equipment. These limitations can be overcome by using a fluorescent-based whole-cell assay and use readily available equipment such as fluorimeters or flow cytometers. Here, we developed complementary fluorescent assays using the membrane potential dye $DiBAC_4(3)$ and the K^+ sensitive indicator APG-1 to evaluate changes in membrane potential ($\Delta\psi$) and intracellular K^+, respectively.

We found that 250 nM $DiBAC_4(3)$ provided a high fluorescent signal in isolated asexual *P. falciparum* trophozoites after 30 min incubation. This condition resulted in a signal-to-noise of 119.28 and a Z'-factor of 0.83 and was used for further analysis of changes in the parasite's membrane potential after treatment with inhibitors. APG-1 (5 µM) resulted in the highest signal-to-background ratio after 60 minutes, that also resulted in high signal-to-noise ratios (276.26) and a Z'-factor of 0.89. Therefore, the two fluorescent probes could successfully be detected in *P. falciparum* parasites and subsequently evaluate changes in $\Delta\psi$ and intracellular K^+.

Putative K^+ channel inhibitors were subsequently evaluated for their potential to inhibit parasite proliferation. The most active inhibitor based on whole-cell activity against the parasite was evaluated with $DiBAC_4(3)$ and APG-1 to determine if the compound causes the changes in $\Delta\psi$ and intracellular K^+ expected following K^+ channel inhibition. We demonstrated that the optimised assays can detect the expected $\Delta\psi$ and intracellular K^+ changes based on the biological effect following treatment with known antimalarial compounds. We also showed that

ion maintenance targets do have distinct profiles that can be used to distinguish between the targets. We envision this assay will be useful for drug mechanism of action studies.

1. Literature review

1.1. Malaria: the disease

Malaria is a disease caused by *Plasmodium* parasites, and these parasites are transmitted to the human host by female *Anopheles* mosquitoes. Although it is a preventable and treatable disease, it still claims the lives of thousands of people a year. Between 2000-2022, effective malaria control strategies resulted in an estimated 11.7 million deaths prevented, but in 2022, approximately 608 000 deaths still occurred due to malaria, with 249 million cases of malaria worldwide (Figure 1.1) (World Health Organization, 2023).

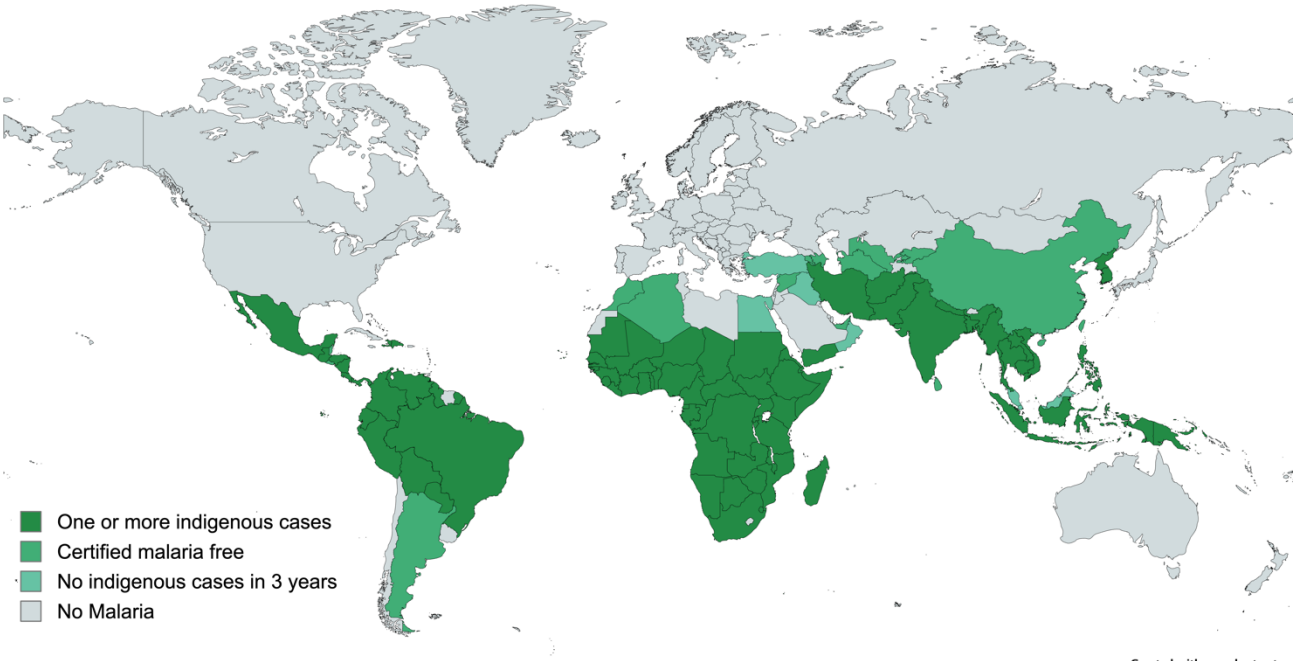

Figure 1.1: Global malaria incidence in 2021. Malaria cases are predominant in Africa, South-East Asia and South America with Africa having the number of cases (95 %). Image adapted from WHO malaria report 2023 and created using MapChart (https://www.mapchart.net/).

Malaria can present as asymptomatic, uncomplicated, or severe malaria. Asymptomatic malaria occurs when malaria parasites are present in the blood of an infected individual, without this person showing symptoms. Patients with asymptomatic malaria can provide a parasite supply for transmission that can lead to symptomatic malaria in other patients (Das et al., 2015). A person with uncomplicated malaria is symptomatic, including fever, nausea, headache, and dizziness, but excludes signs of vital organ dysfunction (Bartoloni and Zammarchi, 2012). Severe malaria presents with the same symptoms as uncomplicated malaria, but in these patients, the disease can also include acute renal failure, severe anaemia and respiratory failure (Bartoloni and Zammarchi, 2012). Malaria can progress rapidly from the first symptom to severe malaria. In adults with no prior exposure to malaria, malaria can

progress to severe malaria in a few days, but in children this could be within 24 hours (Maartens, 2008).

1.2. The life cycle of *P. falciparum* parasites

For malaria to be transmitted, there needs to be an interaction between the host (human), vector (*Anopheles* mosquito) and the parasite (*Plasmodium*) (Rossati et al., 2016). Although there are over 400 *Anopheles* species, only 30-40 of these can spread the parasite (Nicoletti, 2020). In South Africa, the most common species responsible for transmission are *Anopheles funestus, Anopheles arabiensis,* and *Anopheles gambiae* (Kaiser et al., 2021). Of the five *Plasmodium* species that can cause malaria (*Plasmodium falciparum, Plasmodium vivax, Plasmodium malariae, Plasmodium knowlesi*, *Plasmodium ovale curtisi and Plasmodium ovale wallikeri* (Lalremruata et al., 2017), *P. falciparum* has the highest mortality rate (Kavunga-Membo et al., 2018) and is the most widespread in sub-Saharan Africa (Bhatt et al., 2015). And as such *P. falciparum* forms the basis of this study.

Infection occurs when sporozoites are transferred from an infected female *Anopheles* mosquito to the human host during a blood meal (Figure 1.2). Sporozoites are motile and travel in the bloodstream to the liver to infect hepatocytes and initiate the exoerythrocytic developmental cycle (EDC). The first round of asexual replication occurs within hepatocytes (Venugopal et al., 2020), where the sporozoite differentiates to form a multinucleated, exoerythrocytic schizont containing numerous hepatic merozoites (Sturm et al., 2006). These are released back into circulation to infect erythrocytes and initiate the subsequent rounds of asexual replication during the intraerythrocytic developmental cycle (IDC) (Venugopal et al., 2020, Soulard et al., 2015).

After invading the erythrocyte, the parasite changes into a thin indented circle known as the ring stage (Figure 1.2) (Langreth et al., 1978). In this stage, the parasite feeds on small amounts of haemoglobin, also taking up nutrients from the plasma (Spielmann and Beck, 2000). These parasites develop into a trophozoite, where the parasite becomes most metabolically active, undergoes cellular growth while simultaneously modifying the erythrocyte plasma membrane (EPM) to ensure ion and nutrient acquisition (Bannister and Mitchell, 2003). This allows the parasite to grow and develop into a schizont. During schizogony, the intraerythrocytic parasite undergoes three to four rounds of DNA synthesis, mitosis, and nuclear division in the schizont stage to produce 12 – 40 nuclei (Moon et al., 2013). Nuclear segregation and cell division result in daughter merozoites which are released into the bloodstream to infect new erythrocytes and repeat the IDC every 48 hours (Bannister and Mitchell, 2003, Moon et al., 2013). The symptoms associated with malaria are primarily due to

this stage of the life cycle, where the schizonts rupture and the erythrocytes are destroyed (Trampuz et al., 2003).

A small portion (<10 %) of the asexual parasites commit to gametocytogenesis that results in mature gametocytes that can transmit back from host to vector (Figure 1.2) (Talman et al., 2004). Gametocytogenesis in *P. falciparum* takes ~12 days to complete and is distinguished by five different morphological stages (stage I-V). Stage I gametocytes have morphologically similar round shapes to the asexual trophozoite parasite. In stage II gametocytes, a shape change is initiated, and the gametocytes take on a "D" shape. Stage III gametocytes change to a lemon-shaped parasite as the parasite's length is twice its width. Stage IV gametocytes are elongated with pointed ends (Talman et al., 2004, Dixon and Tilley, 2021). The final stage (V) has the falciform or crescent shape that is unique to *P. falciparum* (Chawla et al., 2021). Immature gametocytes (stage I-IV) are sequestered in the bone marrow. Mature male and female gametocytes (stage V) are released back into the blood stream for circulation to be transmitted to a feeding female *Anopheles* mosquito after 2-3 days (Figure 1.2) (Messina et al., 2018).

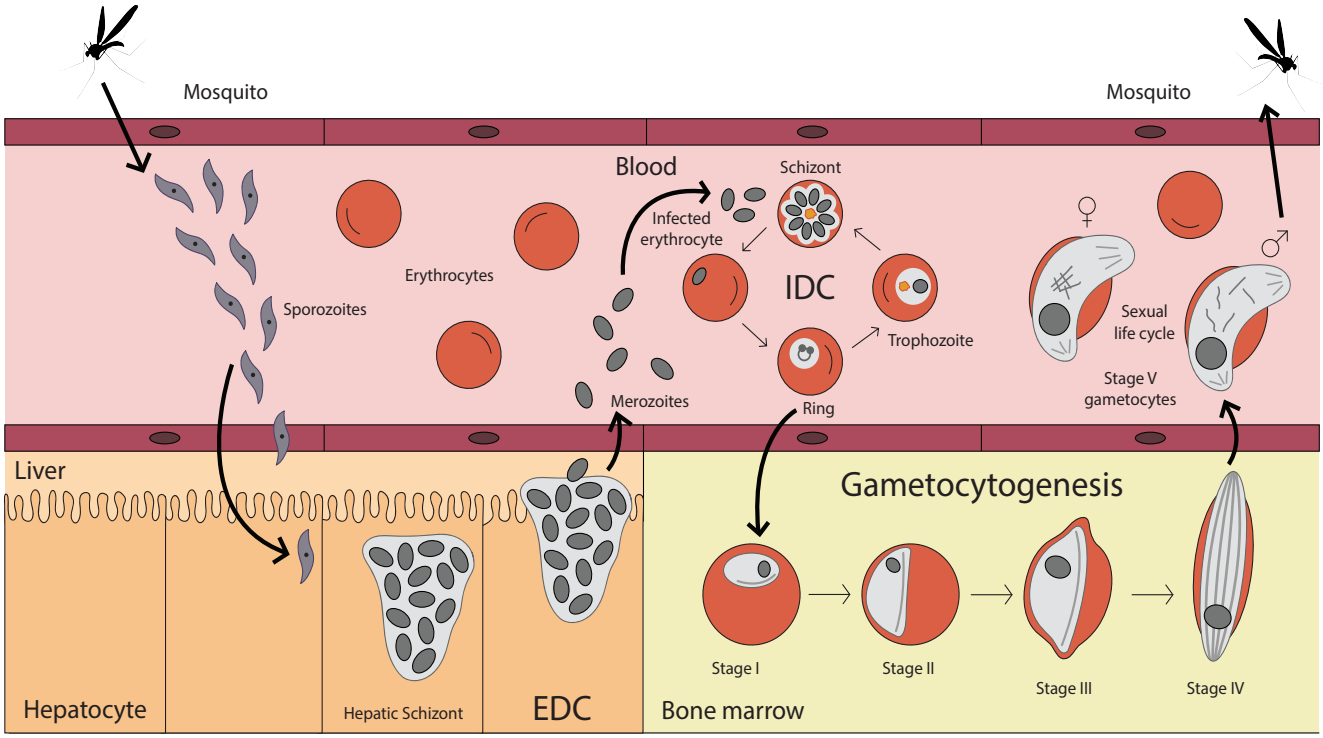

Figure 1.2: *Plasmodium falciparum* life cycle. Sporozoites are release in the blood stream of a human host during the blood meal of an infected female *Anopheles* mosquito. The exoerythrocytic developmental cycle (EDC) is initiated by sporozoites making their way to the liver where they infect the hepatocytes and forms a hepatic schizont that ruptures and releases merozoites. In the blood stream merozoites invades the erythrocytes to start the intraerythrocytic developmental cycle (IDC) where the ring stage parasite will develop into a trophozoite and then a schizont. The schizont bursts and releases merozoites back into circulation to infect new erythrocytes. A small portion of the asexual parasite will commit to gametocytogenesis where they will undergo sexual differentiation. Stage V (mature) gametocytes are transmittable to another mosquito during a blood meal. Figure created with Adobe illustrator.

After uptake by a feeding mosquito, gametocytes differentiate into gametes due to the drop in temperature and the presence of xanthurenic acid within the mosquito midgut (Garcia et al., 1998). Male gametocytes differentiate into 8 flagellated male microgametes, and the female gametocyte differentiates into a single female macrogamete. The microgamete and macrogamete fuse to form a fertile zygote, which develops into a motile ookinete that is able to cross the midgut wall to develop into an oocyst (Grasso et al., 2022). In the oocyst, another round of asexual replication occurs to produce sporozoites. The sporozoites travel to and invade the salivary gland, where they will remain until they can be transmitted to a new host for the cycle to start again (Venugopal et al., 2020).

1.3. Malaria control strategies

The spread of malaria can be controlled by targeting the mosquito vector or the *Plasmodium* parasite itself. Vector control depends on the targeting of mosquito larvae and/or adult mosquitoes (Mpofu et al., 2016). Mosquito control methods include indoor residual spraying (IRS) and the use of long-lasting insecticidal nets (LLINs) (Benelli and Beier, 2017). There are four directly lethal insecticide classes recommended for use with LLINs and IRS, namely, pyrethroids, organochlorines, carbamates, and organophosphates (Fang et al., 2019). Unfortunately, various factors reduced the usefulness of these. Organophosphates and pyrethroids cannot be used in combination or rotation because of cross-resistance. Organochlorides and carbamates have been used in agriculture, and resistance to these insecticide classes has emerged. Organochlorides, carbamates and organophosphates cannot be applied safely at an effective dose with LLINs (Killeen et al., 2017). Therefore, alternative vector control strategies are required. An example of the latter include larviciding which kills immature mosquitoes that are still developing in the water by regularly applying microbial insecticides, chemical insecticides, oils, or larvivores fish (Choi et al., 2019).

Parasite control includes the use of vaccines or chemical compounds to 1) prevent an infection from being established, 2) treat patients with malaria and 3) block transmission. Vaccines can be grouped into three groups: The first group targets the pre-erythrocytic stages, before erythrocytic invasion. These vaccines target the sporozoites and liver stage parasites, aiming to completely prevent infection. A pre-erythrocytic vaccine approved and recommended by the WHO in moderate to high malaria transmission settings is RTS,S/AS01 with an efficacy of 36 % efficacy (El-Moamly and El-Sweify, 2023, Asante et al., 2020, Laurens, 2020). A new pre-erythrocytic vaccine R21/Matrix-M has been approved by WHO and has demonstrated and efficacy of 77 % (Genton, 2023). Erythrocytic vaccines are the second group of vaccines and target the parasites in the blood stages, including merozoites, to reduce the parasite load in an infected person. Both the first and second vaccine groups may thus prevent an infection from

being established. By contrast, the third group of vaccines is transmission-blocking vaccines, targeting gametocytes and gametes, thereby preventing parasite transmission from the human host to the mosquito (Richie and Saul, 2002, El-Moamly and El-Sweify, 2023). Both of the latter groups are still exploratory.

People travelling to malaria-endemic areas, seasonal malaria as well as intermittent preventive treatment makes use of malaria chemoprophylaxis to prevent infection (Ahmad et al., 2021). In South Africa mefloquine, doxycycline, and atovaquone/proguanil is the recommended chemoprophylactic drugs and needs to be taken for 1 week (atovaquone/proguanil) or 4 weeks (mefloquine and doxycycline) after leaving the area (van Zyl, 2018). Seasonal malaria chemopreventation is an effective way of preventing malaria infections in malaria-endemic areas. A course of antimalarials is administered in the malaria season to prevent infections during the peak transmission time (Xu et al., 2023). Sulfadoxine-pyrimethamine (SP) is used as an intermittent preventive treatment of malaria in pregnancy (IPTp) (IPTp-SP) (Nana et al., 2023, Anto et al., 2019). This has been shown to be an effective strategy in which the pregnant woman receives three doses of SP regardless of whether the pregnant woman is infected or not (World Health Organization, 2017). This results in a decrease of pregnant women infected with malaria (Anto et al., 2019).

Chemotherapeutics are used to kill the parasites, thus restricting the infection and the pathological effect (White, 2017). Antimalarials can be clustered into four major classes: antifolates (sulfadoxine and pyrimethamine), quinolines (chloroquine and quinine), artemisinin derivatives (artesunate), and antimicrobials (doxycycline). However, there is resistance against the most commonly used drugs of all four classes mentioned (Cai et al., 2016).

Artemisinin combination therapies (ACTs) is recommended for malaria treatment (Cui et al., 2015, Gatton et al., 2004). Combination therapies are used to reduce the chance of resistance development against both partner drugs. In the case of ACTs, the fast-acting artemisinin component is combined with a slow-acting drug (e.g. lumefantrine) to completely clear an infection (Cui et al., 2015, Cui and Su, 2009). Unfortunately, partial resistance to ACTs has already emerged in Southeast Asia and East Africa (Hanboonkunupakarn et al., 2022). Resistance to ACTs emphasises the need for new chemotherapeutics and, therefore, a greater understanding of the biology of parasites.

1.4. Regulation of ion transport and membrane potential in *P. falciparum* parasites

P. falciparum parasites are surrounded by three membranes: the EPM, parasitophorous vacuolar membrane (PVM), and the parasite plasma membrane (PPM) (Counihan et al., 2021). Nutrients taken from the surrounding environment must cross these three membranes to reach the parasite. Although the EPM has substrate specific transporters, not all substrates necessary for parasite survival can be acquired through these transporters from the human host. To increase the EPM permeability, trophozoite stage parasites (15-20 hours post invasion (hpi)) modifies the EPM to create new permeation pathways (NPPs) (Counihan et al., 2021, Mauritz et al., 2011). NPPs increase the permeability of infected erythrocytes to a range of small molecular weight solutes such as sugars, amino acids, and ions (Kirk, 2015). NPPs have the characteristics of an anion-selective channel and are referred to as *Plasmodium* surface anion channel (PSAC). Soluble macromolecules cross the PVM via a cation and anion permeable channels that acts as a sieve. The transport of nutrients across the PVM is only limited by the size (<1.4 kDa) of the solute and the diffusion coefficient (Counihan et al., 2021). The substrate that reaches the PPM can then be transported in to the parasite via the transporters on the PPM (Martin, 2020).

Once the *P. falciparum* parasite has entered the erythrocyte, the environment surrounding the parasite changes from high [Na^+]/ low [K^+] in blood plasma to low [Na^+]/ high [K^+] in the erythrocyte cytosol (Figure 1.3 A) (Lee et al., 1988). This low [Na^+]/ high [K^+] in the uninfected erythrocyte is maintained by the human Na^+/K^+ ATPase that transports Na^+ out of the erythrocyte and K^+ into the erythrocyte (Radosinska and Vrbjar, 2016). The NPPs mediate a change in Na^+ and K^+ concentrations in the infected erythrocyte, thereby altering the surrounding environment of the parasite in the erythrocyte to a high [Na^+]/ low [K^+] environment, similar to what the parasite experienced in blood plasma (Figure 1.3 B) (Mauritz et al., 2011).

The high cytosolic [Na^+] in the infected erythrocyte cytosol results in a large inwardly directed [Na^+] gradient into the parasite. PfATP4 actively exports Na^+ against the inward gradient into the erythrocytic cytosol to counter the inward leakage of Na^+ into the parasite down its concentration gradient (Spillman et al., 2013b). PfATP4 is a P-type ATPase and is located on the plasma membrane of the parasite. The export of Na^+ is coupled with the import of H^+, placing a significant acid load on the parasite that must be countered by the export of H^+ (Spillman et al., 2013a). The vacuolar-type H^+-ATPase (V-type-ATPase) can be found on the PPM and is the major source of H^+ export. The export of H^+ also results in the inward negative membrane potential ($\Delta\psi$) across the plasma membrane. The $\Delta\psi$ is modulated by the influx of

K^+ due to electrodiffusion against the [K^+] gradient via the K^+ channels, resulting in a final membrane potential of -95 mV (Figure 1.3 B) (Allen and Kirk, 2004).

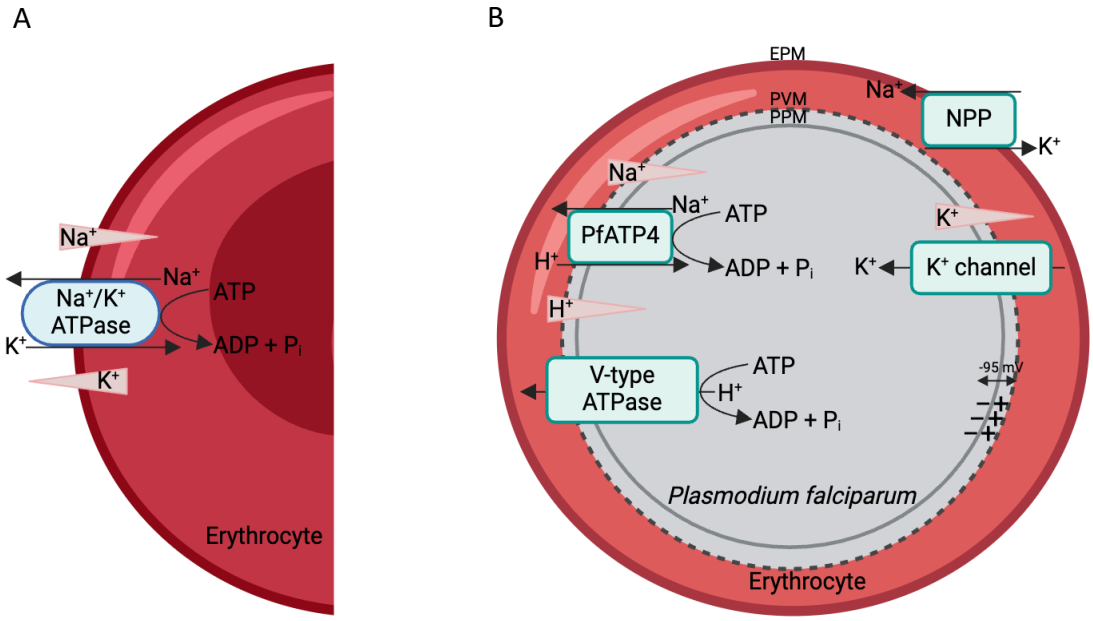

Figure 1.3: *P. falciparum* ion and membrane potential regulation. A) Low Na^+, high K^+ cytosol in the uninfected erythrocyte is maintained by the human Na^+/K^+ ATPase. The Na^+/K^+ ATPase exports Na^+ against its concentration gradient while importing K^+ against its concentration gradient. B) Small molecular weight solutes, including ions from the blood plasma cross the erythrocyte plasma membrane (EPM) via the new permeation pathways (NPPs). The solutes reaching the parasitophorous vacuolar membrane (PVM) can cross this membrane via the sieve-like channels on the PVM. PfATP4 actively pumps Na^+ out of the parasite cytosol against the inward Na^+ gradient, while also pumping H^+ into the cytosol of the parasite. The V-type-ATPase is responsible for the export of H^+ out of the parasite and into the erythrocyte. The export of H^+ results in the inward negative membrane potential (Δψ) across the parasite plasma membrane (PPM). The Δψ is regulated by the influx of K^+ against the K^+ concentration gradient via the K^+ channels resulting in a final membrane potential of -95 mV. The figure was generated on BioRender under the basic license for educational purposes and basic design.

1.5. Inhibition of ion transport and Δψ regulation as antiplasmodial target

Large-scale phenotypic screening, where a compound's effect on parasite proliferation was tested without prior knowledge of the molecular target, has been very successful in discovering new antimalarial drug candidates (Yang et al., 2021). The disadvantage of this approach is that, without further studies and biochemical assays, the mode of action of the compound (MoA) remains unknown (Plouffe et al., 2008). Target identification requires extensive biological investigations. For example, the target of an active compound can be identified by *in vitro* evolution and whole-genome analysis (IVEWGA) to identify proteins that mutate in response to the drug (Yang et al., 2021). This will identify either the protein responsible for resistance and/or the actual target. Targeted MoA investigations can thus be based on this information.

Two such identified compounds include triaminopyrimidine ZY-19489 that completed Phase I investigations in 2022 (Barber et al., 2022), and the spiroindolone KAE609 (Cipargamin) currently in Phase II trials (Schmitt et al., 2022). Antimalarials belonging to the triaminopyrimidines (TAPs) class has nanomolar activity with a long half-life against *P. falciparum* resistant strains. IVEWGA identified a mutation in the V-type-ATPase subunit D as a potential resistance mechanism for TAPs (Hameed et al., 2015). Treatment of parasites with the generic V-type-ATPase inhibitor Bafilomycin A_1 leads to an increased [H^+] of the parasite's cytoplasm (Figure 1.4) (Hayashi et al., 2000, Saliba and Kirk, 1999). Radiolabelled assays have also shown that Bafilomycin A_1 leads to membrane depolarisation (Allen and Kirk, 2004). It is possible that TAPs also lead to depolarisation, but the direct effect of TAPs on the Δψ had not yet been measured at the beginning of the study and would require a suitable Δψ assay.

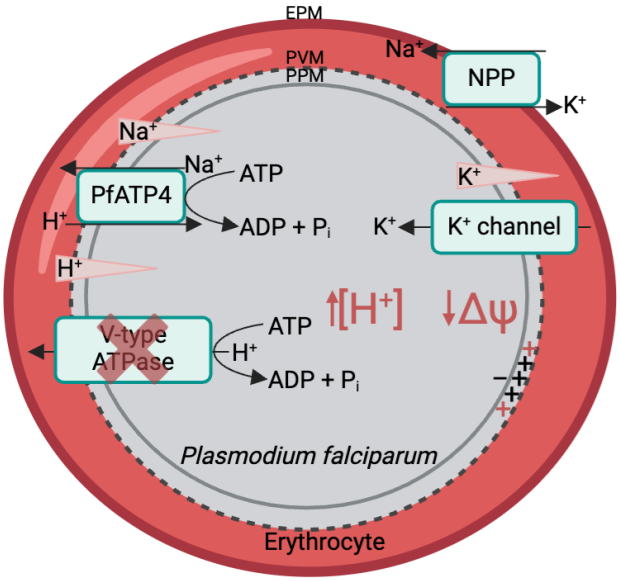

Figure 1.4: The biological effect of V-type ATPase inhibition in *P. falciparum*. Treatment of parasites with the V-type-ATPase inhibitor Bafilomycin A_1 leads to the increase of parasite cytoplasmic acidification and a decrease in Δψ (depolarised, less negative). The figure was generated on BioRender under the basic license for educational purposes and basic design.

With regards to spiroindolone KAE609, exposure resulted in mutations in PfATP4 (Rottmann et al., 2010), later identified as the target of KAE609 (Spillman et al., 2013b). Inhibition of PfATP4 activity results in a characteristic cellular response: with inhibition of Na^+ export and H^+ import causing cytosolic alkalinisation (Lehane et al., 2014). Parasites treated with PfATP4 inhibitors show an immediate disruption of Na^+ and pH homeostasis (Figure 1.5) (Spillman et al., 2013b), leading to detrimental swelling of the entire infected cell (Spillman and Kirk, 2015). The characteristic cellular response observed following PfATP4 inhibition was subsequently used in biochemical assays to identify other chemical classes that inhibit PfATP4 without having to use IVEWGA (Lehane et al., 2014). By measuring intracellular Na^+ levels and pH changes with fluorescent Na^+ and pH indicators, six compounds out of the set of 400

compounds included in the Malaria Box (www.mmv.org/malaria-box) were confirmed as PfATP4 inhibitors (Van Voorhis et al., 2016).

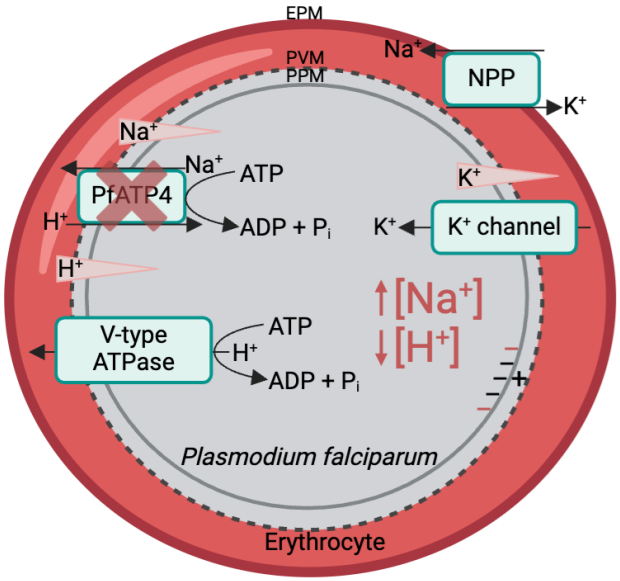

Figure 1.5: Biological effect of PfATP4 inhibition. When PfATP4 is inhibited, the exchange of H^+ for Na^+ is stopped, causing an increase in cytosolic pH. The figure was generated on BioRender under the basic license for educational purposes and basic design.

1.6. Evidence for K^+ regulation as antiplasmodial target

K^+ is the most abundant intracellular cation, essential for a wide range of functions. Given the sensitivity of *P. falciparum* parasites to compounds that inhibit proteins involved in ion homeostasis, it stands to reason that inhibition of K^+ channels will most likely result in cell death (Figure 1.6). K^+ channel blocking with Cs^+ or Ba^{2+} prevents K^+ from entering the parasite to offset the highly negative $\Delta\psi$ generated by the export of H^+ by the V-type ATPase (Figure 1.6), thereby leading to membrane hyperpolarisation (more negative) (Allen and Kirk, 2004).

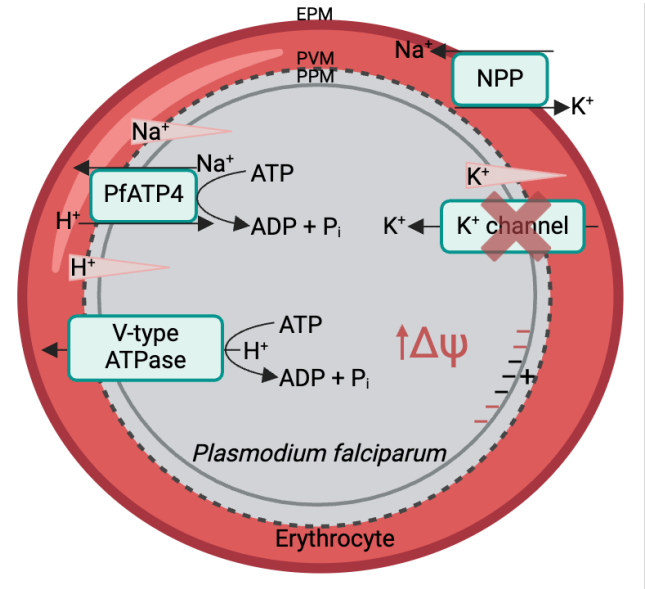

Figure 1.6: *P. falciparum* K^+ channel inhibition. In the presence of K^+ channel inhibitors the parasite is not able to import K^+ into the cell. This results in the Δψ becoming more negative due to the V-type ATPase activity. The figure was generated on BioRender under the basic license for educational purposes and basic design.

As expected, inhibitors proven to inhibit K^+ channels in other organisms (Table 1.1) inhibit the proliferation of asexual parasites (Waller et al., 2008a, D'Alessandro et al., 2015, Schmitt et al., 2022). While interference with K^+ levels has been proposed as the mode of action of these inhibitors, none of the studies to date determined the direct effect on intracellular K^+ levels. There are several limitations to the inhibitors tested. Although these inhibitors have been used as K^+ channel inhibitors in other organisms, some of these have additional non K^+ channel targets. Of the previously tested compounds that only target K^+ channels, some do not necessarily target the class of K^+ channels expressed in *P. falciparum*. The *P. falciparum* genome encodes for putative voltage-gated (Kv) and big conductance Ca^{2+}-activated K^+ (BK) channels (Waller et al., 2008a, Ellekvist et al., 2004), and inhibitors should be geared towards these classes.

Table 1.1: Summary of K^+ channel inhibitors previously showed to inhibit *P. falciparum* proliferation, tested with the [^{3}H]-hypoxanthine incorporation assay.

Compound	Targets(s)	IC_{50} value
Quinine	Interferes with haemoglobin digestion	71 ± 4 nM
Quinidine	Interferes with haemoglobin digestion	36.5 ± 1.3 nM
Apamine	ATP-type Ca^{2+}-activated K^+ channels	ND
Bicuclline methiodidle	Gamma-aminobutyric acid receptor and Ca^{2+}-activated K^+ channels	79.3 ± 2.9 µM
Charybdotoxin	Ca^{2+}-activated K^+ channels and voltage-gated K^+ channels	ND
Clotrimazole	inhibits haem-peroxidase	0.060 ± 0.001 µM
Haloperidol	Inwardly rectifying K^+ channels and voltage-gated K^+ channels	4.29 ± 0.17 µM
Tubocurarine chloride	Ca^{2+}-activated K^+ channels	129 ± 3.2 µM
Trifluoperazine hydrochloride	CDPK4 inhibitor	45 ± 1 µM
Verruculogen	Ca^{2+}-activated K^+ channels	ND

There are however more direct lines of evidence for the importance of K^+ regulation in the form of ionophore studies. Ionophores form hydrophilic pores in the membrane to allow selected cations to pass through the membrane, disrupting the transmembrane concentration gradient (David and Rajasekaran, 2015). K^+ ionophores have low nanomolar activity against *P. falciparum* asexual parasite proliferation (Table 1.2). Boromycin, monensin, salinomycin, and nigericin were also tested against gametocytes with low nanomolar activity, indicating that the use of K^+ ionophores are detrimental to both asexual parasites and gametocytes (D'Alessandro et al., 2015, de Carvalho et al., 2021). Therefore, interference with K^+ maintenance may be an avenue for new antiplasmodial compounds; however, the effect of these compounds on *P. falciparum* K^+ levels must first be proven.

Table 1.2: Summary of ionophores previously used in *P. falciparum,* resulting in parasite death.

Ionophore Name	Targets(s)	Assay	IC_{50} value	References
Boromycin	K^+ ionophore	ELISA	0.9 ± 0.1 nM (Asexual parasites)	(de Carvalho et al., 2021)
		ELISA	9 ± 4 nM (Stage V gametocyte)	
Monensin	Exchanges H^+ for K^+ or Na^+	pLDH	1.0 ± 0.2 nM (Asexual parasites)	(Adovelande and Schrevel, 1996, D'Alessandro et al., 2015)
		pLDH	1.9 ± 1.3 nM (Stage II-III gametocyte)	
		pLDH	5.7 ± 1.1 nM (Stage IV-V gametocyte)	
Valinomycin	K^+ ionophore	[^{3}H]-hypoxanthine incorporation assays	4.76 nM	(Lim et al., 2012, Gumila et al., 1996)
Salinomycin	K^+ ionophore	pLDH	21.9 ± 12.3 nM (Asexual parasites)	(D'Alessandro et al., 2015)
		pLDH	14.5 ± 7.4 nM (Stage II-III gametocyte)	
		pLDH	6.3 ± 1.7 nM (Stage IV-V gametocyte)	
Nigericin	Electroneutral exchange of K^+ for H^+	pLDH	1.8 ± 1.0 nM (Asexual parasites)	(D'Alessandro et al., 2015, Pressman, 1968)
		pLDH	2.7 ± 1.2 nM (Stage II-III gametocyte)	
		pLDH	0.9 ± 0.4 nM (Stage IV-V gametocyte)	
Gramicidin	Na^+ and K^+ ionophore	[^{3}H]-hypoxanthine incorporation assays	0.27 ± 0.14 nM	(Bharti et al., 2019, Otten-Kuipers et al., 1995)
Maduramicin	Na^+ ionophore	[^{3}H]-hypoxanthine incorporation assays	2.67 nM	(Das et al., 2016, Raza et al., 2018)
Lonomycin	Ca^{2+} ionophore	pLDH	13 nM	(Morgan and Jacob, 1994, Otoguro et al., 2001)
Lasalocid	Monovalent and divalent ionophore cations	pLDH	29 nM	(Mahtal et al., 2020, Otoguro et al., 2001)
Narasin	Monovalent cations	pLDH	1.6 nM	(Cybulski et al., 2015, Otoguro et al., 2001)
Calcimycin	Ca^{2+} ionophore	pLDH	1.2 µM	(Reed and Lardy, 1972, Otoguro et al., 2001)

1.7. Ion and Δψ detection assays

Different techniques have been used to detect Na^+ and K^+ levels in infected erythrocytes, including flame photometry (Overman, 1948), ion-sensitive electrodes (Pillai et al., 2013) and high performance liquid chromatography (HPLC) (Winterberg and Kirk, 2016). However, these techniques require specialised equipment, sample preparation and/or radiolabelled probes. An example of the use of HPLC was to determine the intracellular Na^+ and K^+ levels of untreated versus treated *P. falciparum* parasites with KAE609, and the Δψ was measured using the K^+ congener ^{86}Rb (Ellekvist et al., 2008).

An alternative may be fluorescent dyes, which are compounds with intense fluorescent properties that can absorb and emit light within the visible region of the electromagnetic spectrum (Christie, 2011). Fluorescent dyes are a powerful tool that has been used for biosensing and bioimaging due to their high sensitivity and specificity (Zhu et al., 2016). Compared to other techniques, fluorescent dyes have an advantage because they allow fast detection with high selectivity, are less invasive allowing use in intact cells, are easy to use and use readily available equipment for detection (Nagano, 2010, Yoon et al., 2021, Oliveira et al., 2018).

In *Plasmodium* parasites, parasite cytosolic Na^+ concentrations have been measured using a fluorescent Na^+ sensitive dye 'sodium binding benzofuran isopthalate' (SBFI) (Spillman et al., 2013b). SBFI comprises of fluorophores that are linked to a crown ether which confers selectivity for Na^+ (Minta and Tsien, 1989). This is a ratiometric dye with an 18-fold higher selectivity for Na^+ over K^+, with an excitation of 340 nm and emission of 500 nm (Iamshanova et al., 2016, Minta and Tsien, 1989). SBFI has been used to investigate the effect of PfATP4 inhibition on Na^+ levels in *P. falciparum* (Spillman et al., 2013b), as well as to identify compounds that may inhibit PfATP4 based on the effect on Na^+ levels (Dennis et al., 2018b, Dennis et al., 2018a, Lehane et al., 2014).

Some probes have been developed that respond to K^+ ions, however, these are not efficient in selectively measuring K^+ in the presence of other monovalent cations (Boyd et al., 2021). 'Potassium binding benzofuran isophalate' (PBFI) is a fluorescent dye that is used to determine intracellular K^+ concentrations. PBFI has two benzofuran isophalate fluorophores connected to the diazacrown ether, which confers selectivity for K^+. PBFI is only 1.5-fold more selective to K^+ than Na^+ (Meuwis et al., 1995). PBFI affinity for K^+ (Kd = 8 mM) provide low sensitivity for K^+ in intracellular environments that have a concentration of K^+ higher than 100 mM (Rimmele and Chatton, 2014). A disadvantage however is PBFI does not work on readily available equipment, as it requires far-UV excitation, which can also cause photodamage (Rana et al., 2019).

Asante potassium green (APG) based dyes are fluorescent K^+ probe used to determine K^+ levels in a cell (Rana et al., 2019). The acetoxymethyl ester creates a hydrophobic molecule that allows the dye to enter the cell by diffusion. Cytosolic esterases cleaves the acetoxymethyl ester, charging the dye and trapping the hydrophilic dye inside the cell (Jobsis et al., 2007). In contrast to PBFI that needs UV excitation, APG has an excitation peak around 500 nm, indicating that UV excitation is not needed (Rana et al., 2019). APG also overcomes the poor loading efficiency typically seen when using PBFI (Rimmele and Chatton, 2014). Compared to PBFI, APG is only slightly influenced by Na^+ at intracellular levels (Rimmele and Chatton, 2014).

Bis(1,3-Dibutylbarbituric Acid) Trimethine Oxonol ($DiBAC_4(3)$ is a slow, voltage-sensitive Δψ fluorescent dye previously used in *P. falciparum* (Allen and Kirk, 2004). The negatively charged $DiBAC_4(3)$ distributes between the outer and inner leaflet of the membrane, based on the Δψ. Membrane depolarisation allows for the accumulation of the negatively charged dye in the cell, resulting in an increase in signal while hyperpolarisation results in a decreased signal (Yamada et al., 2001). $DiBAC_4(3)$ has been used to measure Δψ in both uninfected erythrocytes (Moersdorf et al., 2013) as well as *P. falciparum* parasites that have been isolated from the erythrocyte (Allen and Kirk, 2004).

1.8. Changes in ion and Δψ fluorescent dye signals can be predicted based on known biological effects

There are several possible scenarios that can be observed if antiplasmodial compounds target proteins involved in ion and Δψ regulation (Figure 1.7). Inhibition of the V-type ATPase results in a decrease in H^+ export and PPM depolarisation (less negative Δψ) (Hayashi et al., 2000, Allen and Kirk, 2004). Therefore, there will be less of an electrical gradient that can pull K^+ into the parasite against the K^+ concentration gradient, resulting in lower intracellular K^+ levels (Figure 1.7 A). On the contrary, inhibition of either PfATP4 or K^+ uptake should result in a more negative Δψ (Figure 1.7 B and C). Inhibition of PfATP4 prevents the exchange of intracellular Na^+ for extracellular H^+. However, since the V-type ATPase is still active, there is a constant export of H^+ that is no longer replenished, leading to hyperpolarisation of the PPM (more negative Δψ) (Figure 1.7 B). This hyperpolarisation may lead to increased K^+ influx. By contrast, preventing K^+ influx into the parasite cytosol while maintaining V-type ATPase mediated H^+ export will also hyperpolarise the PPM but will lead to a decrease in K^+ levels (Figure 1.7 C). To distinguish between these scenarios, the effect on not only intracellular K^+ but also Δψ must be measured. Membrane hyperpolarisation with increased K^+ levels, indicate PfATP4 inhibition, while membrane hyperpolarisation with a decrease in K^+ levels indicate K^+

channel inhibition. By contrast membrane depolarisation with a decrease in K^+ levels, indicate V-type ATPase inhibition (Figure 1.7 D).

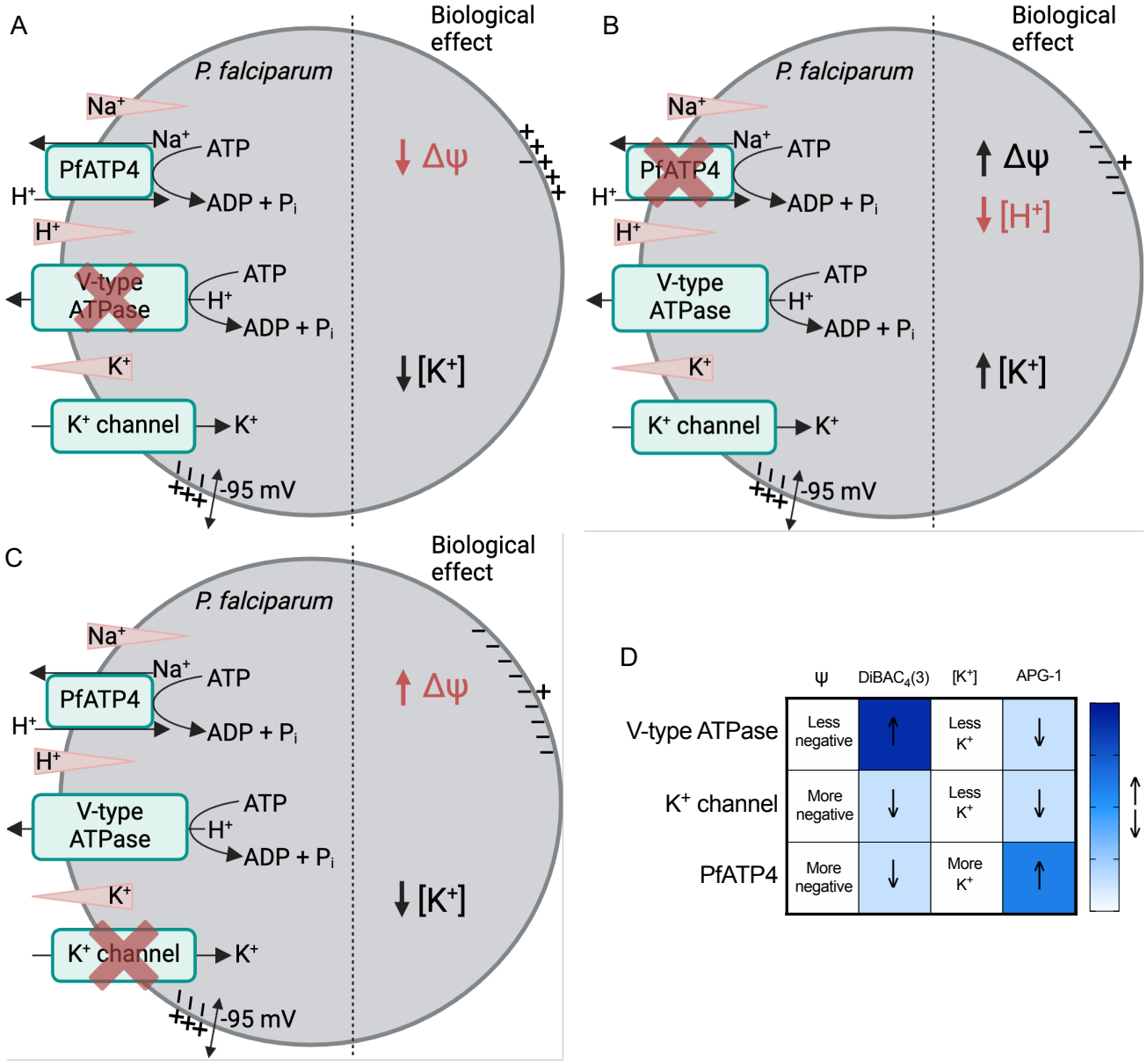

Figure 1.7: Distinct profiles of ion maintenance targets. Proven biological effects are indicated in red while expected biological effects are indicated in black. A) Inhibition of V-type ATPase results in H^+ export being blocked, the Δψ becomes more positive, and less K^+ flows into the parasite. B) Inhibition of PfATP4 leads to blocked import of H^+, the Δψ becomes more negative and more K^+ flows into the parasite. C) K^+ channel inhibition results in a decrease in K^+ flow into the parasite and the Δψ becomes more negative. D) Heatmap representation of expected changes in $DiBAC_4(3)$ and APG-1 fluorescence following inhibition ofion maintenance proteins. $DiBAC_4(3)$ signal increases as the Δψ becomes more positive, and decrease if Δψ becomes more negative. APG-1 fluorescence increase with increased intracellular K^+, and decrease with a decrease in intracellular K^+. Figures were generated on BioRender under the basic license for educational purposes and basic design.

In this study, we propose to develop simple fluorescence-based assays to determine changes in Δψ and intracellular K^+ levels of *P. falciparum* after treatment with antiplasmodial compounds. This assay will not only be useful in confirming that the effect of putative K^+ channel inhibitors and ionophores are due to perturbing K^+ levels, but will also be used to differentiate between the inhibition of different proteins involved in ion regulation.

2. Aim, Hypothesis and Objectives

2.1. Hypothesis

APG-1 and $DiBAC_4(3)$ fluorescent dyes can measure Δψ and intracellular K^+ levels in isolated *P. falciparum* parasites.

2.2. Aim

Establish semiquantitative fluorescent assays to detect changes in membrane potential and intracellular K^+ levels in isolated *P. falciparum* parasites.

2.3. Objectives

I. Determine if $DiBAC_4(3)$ fluorescence responds to Δψ changes.

II. Establish if APG-1 fluorescence responds to changes in intracellular K^+ levels.

III. Identify a control K^+ channel inhibitor for use in Δψ and intracellular K^+ assays.

IV. Determine if ion maintenance proteins have responses with $DiBAC_4(3)$ and APG-1.

2.4. Research outputs

Thomas, J., Claassen, E., Birkholtz, L., Niemand, J. Investigating the functional relevance of K^+ channels in asexual *Plasmodium falciparum* parasites. 7th South African Malaria Research Conference. Poster presentation. Virtual, August 2022.

Thomas, J., Claassen, E., Birkholtz, L., Niemand, J. Assante Potassium Green-1 as a tool for analysing changes in *Plasmodium falciparum* intracellular K^+ levels. 4th H3D symposium. Poster presentation. Stellenbosch, South Africa, October 2022

Thomas, J., Claassen, E., Birkholtz, L., Niemand, J. A fluorescence-based assay of K^+ levels in intraerythrocytic *Plasmodium falciparum* parasites. 8th South African Malaria Research Conference. Poster presentation. Pretoria, South Africa, August 2023

Thomas, J., Claassen, E., Birkholtz, L., Niemand, J. Semiquantitative fluorescent methods to detect changes in membrane potential and intracellular K^+ levels in *Plasmodium falciparum* distinguish between different ion maintenance targets. MPM XXXIV 2023. Poster presentation. Woods Hole, USA, September 2023

3. Methods and Materials

3.1. Identification of K^+ channel inhibitors

Given that the K^+ channels of *P. falciparum* fall into the classes of Kv and Bk (Waller et al., 2008a, Ellekvist et al., 2004), Kv and BK channel inhibitors with proven K^+ channel inhibition in other organisms were identified. Inhibitors that targeted additional ion channels, apart from K^+ channels, were removed from the list as well as K^+ channel inhibitors that does not target Kv or BK channels. Inhibitors that had a molecular weight greater than 500 g/mol were also removed. This resulted in six K^+ channel inhibitors investigated in this study: Paxilline (Cayman chemical, USA), AUT1 (Cayman chemical, USA), XE-991 (Sigma-Aldrich, USA), GAL_021 (Cayman chemical, USA), 4-aminopyridine (Sigma-Aldrich, USA) and 3,4-diaminopyridine (Sigma-Aldrich, USA).

3.2. Intraerythrocytic *P. falciparum* parasite culturing

3.2.1. Ethical clearance statement

All experiments requiring *P. falciparum* parasites were performed at the University of Pretoria in the Malaria Parasite Molecular Laboratory (M^2PL), a biosafety level 2 (BSL2) certified facility (registration number: 39.2/University of Pretoria-19/160). All *in vitro* parasite cultivation and the use of human blood were covered by an umbrella ethics clearance for the SARChi program under Prof. Lyn-Marié Birkholtz (NAS ethics approval no: 180000094). This project was approved under NAS ethics clearance number: NAS026/2022.

P. falciparum drug sensitive strain NF54, chloroquine resistant strain Dd2 and multidrug resistant strain K1 parasites were obtained from BEI resources (https://www.beiresources.org). These parasites were cultured in human erythrocytes (blood types A+ or O+) using standard procedures (Trager and Jensen, 1976) at 5 % haematocrit in complete culture medium [RPMI-1640 culture medium (Sigma-Aldrich, USA), supplemented with 0.0024 mg/mL gentamycin (HyClone, USA), 0.2 % (w/v) glucose (Merck, Germany), 25 mM HEPES pH 7.2- 7.5 (Sigma-Aldrich, USA), 200 µM hypoxanthine (Sigma-Aldrich, USA), 32.81 mM sodium bicarbonate (Sigma-Aldrich, USA) and completed with 5 g/L Albumax II (Life technologies, USA)]. Cultures were maintained between 4-6 % parasitaemia under hypoxic conditions of 90 % N_2, 5 % CO_2, 5 % O_2 (Afrox, South Africa) with rotation at 60 rpm and at 37 °C to allow single merozoite invasion. Parasitaemia was calculated by the number of infected erythrocytes divided by the total number of erythrocytes. If the parasitaemia was 4 % or more non-infected erythrocytes and culture media were added.

3.2.2. RapiDiff visualization of *P. falciparum* parasites

Thin smears of intraerythrocytic *P. falciparum* parasite cultures were fixed with methanol and stained using RapiDiff (Merck, South Africa) for visualisation. Stained slides were used to determine the parasitaemia using a YS2-H Nikon light microscope (Nikon, Japan) with oil immersion at 1 000x magnification. The Nikon Eclipse 50i microscope (Nikon, Japan) was used to take pictures of the parasites and analyse them on the NIS-Element software F package version 3.0 (Nikon, Japan).

3.2.3. Synchronisation of asexual *P. falciparum* parasites

Asexual *P. falciparum* parasite cultures comprising of at least 2 % ring-stage parasites were synchronised using 5 % (w/v) D-sorbitol (Sigma-Aldrich, USA) (Lambros and Vanderberg, 1979). Due to the NPPs formed in the trophozoite and schizont stage, these parasites are more permeable to D-sorbitol resulting in the lysis of these parasite stages. This results in a majority synchronised ring-stage culture. Culture samples were incubated with D-sorbitol for 10 min at 37 °C and then centrifuged for 2 min at 3500 x*g*. Afterward, the culture was washed twice with incomplete culture medium to ensure excess D-sorbitol and parasite debris were removed. The culture was then readjusted to a 5 % haematocrit with non-infected erythrocytes and complete culture medium.

3.3. SYBR Green I fluorescence assay to measure *in vitro* activity of compounds against asexual *P. falciparum* parasite proliferation

The SYBR Green I assay was used to measure the proliferation of *in vitro* intraerythrocytic *P. falciparum* NF54, Dd2, and K1 parasites after treatment with compounds. Anti-plasmodial activity of the potential K^+ channel inhibitors Paxilline (Sigma-Aldrich, USA and Cayman chemical, USA), AUT1 (Cayman chemical, USA), XE-991 (Sigma-Aldrich, USA), GAL_021 (Cayman chemical, USA), 4-aminopyridine (Sigma-Aldrich, USA) and 3,4-diaminopyridine (Sigma-Aldrich, USA), was determined using the SYBR Green I fluorescence-based assay. SYBR Green I intercalates into the minor groove of double-stranded DNA. This assay can be used to specifically determine parasite double-stranded DNA as a proxy for parasite proliferation, seeing that erythrocytes do not contain nuclear material. The activity of the known V-type ATPase inhibitor concanamycin A (van Schalkwyk et al., 2010) (Glentham Life Sciences, UK) and the known PfATP4 inhibitor KAE609 (Spillman and Kirk, 2015) was also validated on the strains used here, and these compounds would serve as controls for inhibition of the two proteins.

In a 96-well plate, a 2-fold serial dilution of the compounds was performed in complete culture medium using chloroquine (0.5 µM) as a background control and untreated parasites as a positive control for proliferation. A parasite suspension was made using a synchronised asexual parasite culture (>95 % ring-stage) at 1 % parasitaemia and 2 % haematocrit. The parasite suspension was added to each well in a 1:1 ratio, resulting in a final haematocrit of 1 %. The plates were incubated at 37 °C in a stationary incubator for 96 h under hypoxic conditions (90 % N_2, 5 % CO_2, 5 % O_2).

Following incubation, samples were resuspended in a 1:1 ratio in a 96-well plate with SYBR Green I lysis buffer [5 mM EDTA (Sigma-Aldrich, USA), 0.008 % (w/v) saponin (Sigma-Aldrich, USA), 20 mM Tris (Sigma-Aldrich, USA) pH 7.5, 0.08 % (v/v) Triton X-100 (Sigma-Aldrich, USA)] supplemented with 0.002 % (v/v) SYBR Green I (Invitrogen, USA) and incubated for 1 h in the dark at room temperature. Fluorescence was measured using a Fluoroskan Ascent FL microplate fluorimeter (Thermo Scientific, USA; excitation 490 nm, emission 520 nm). Excel was used to analyse the data where the background was subtracted, and the data were normalised relative to the positive control for proliferation. Data were represented as a dose-response curve using GraphPad 9.2.0 (GraphPad Software, USA) showing the standard error of the mean (S.E.). Data were used from three independent experiments, each of which was performed in technical triplicates.

3.4. Measurement of changes in the membrane potential using $DiBAC_4(3)$

Late-stage trophozoites (34-37 hpi) were isolated using saponin (0.05 % v/v, Sigma-Aldrich, USA) inverted 5 times and then centrifuged for 2 min at 3260 x*g* in a SL 8R centrifuge (Thermo Scientific, USA). The supernatant was removed, and the pellet washed 3 times with normal malaria saline [125 mM NaCl (Glentham Life Sciences, UK), 5 mM KCl (Merck, Germany), 25 mM HEPES (Sigma-Aldrich, USA), 20 mM Glucose (Merck, Germany) and 1 mM $MgCl_2$ (Merck, Germany), pH 7.1] (Saliba et al., 1998) after which the isolated parasites were resuspended in 1 mL malaria saline. The number of isolated parasites was determined using an improved Neubauer haemocytometer and adjusted to 3 x 10^7 parasites/mL. $DiBAC_4(3)$ (Sigma-Aldrich, USA) was added to the parasite suspension (final concentration 250 nM) and then incubated in a shaking incubator (160 rpm) (MRC LM-570 incubator, Israel) for 30 min (Moersdorf et al., 2013) at 37 °C in the dark. Subsequently, the samples were transferred to a 96-well plate and the fluorescence was read using a Fluoroskan Ascent FL microplate fluorimeter (Thermo Scientific, USA; excitation 490 nm, emission 520 nm). Malaria saline, with 0.025-0.2 % v/v DMSO as vehicle control, was used as background fluorescence control. Excel was used to analyse the data where the background was subtracted, and the data were normalised relative to the untreated parasites.

To obtain the optimal concentration of $DiBAC_4(3)$ to be used in an assay, the same method as mentioned above was used with different concentrations of $DiBAC_4(3)$ (Table 3.1). Likewise, different incubation times of $DiBAC_4(3)$ (final concentration 250 nM) stained parasites were tested following the same procedure.

Table 3.1: Optimal concentration and incubation time of $DiBAC_4(3)$ for *P. falciparum*.

	$DiBAC_4(3)$ concentration (nM)	Incubation time (min)
Optimal concentration	1.5	30
	3	
	6	
	12	
	24	
	250	
Optimal incubation time	250	30
		60
		90

To determine the effect of different compounds on Δψ, different experimental conditions were used as follows: Ionophores (Gramacidin, Valinomycin, Nigericin, and Salinomycin) were tested at a single concentration of 5 µM. Paxilline was used at different concentrations (12.5 µM, 25 µM, 50 µM, 100 µM and 150 µM) to determine if this K^+ channel inhibitor results in a dose dependent response in Δψ. For all other experiments, Paxilline was used at a single concentration of 50 µM. The V-type ATPase inhibitor Concanamycin A was tested at 200 nM while the PfATP4 inhibitor KAE609 was used at 1 µM. The predicted K^+ channel inhibitors Tubocurarine chloride, Apamine and 4-aminopyridine, the known antimalarials Chloroquine, Dihydroartemisinin, Pyrimethamine, Sulfadoxine, Quinine, and antiplasmodial compounds Clemizole (MMV002015) and MMV1634391 were all tested at 10 µM. Trophozoites isolated using saponin (0.05 % v/v) were resuspended to 3 x 10^7 parasites/mL and incubated for 15 min with the above compound(s) before $DiBAC_4(3)$ (final concentration 250 nM) was added. After the dye was added, the samples were incubated for 30 min before fluorescence was measured. Fluorescence was measured and data analysed as above.

3.5. Changes in K^+ levels using APG-1

Of the three APG dyes APG-1 will be used to determine changes in intracellular K^+ levels based on the Kd value (Kd= 50 mM) and the high intracellular K^+ levels inside the parasite cytosol. Isolated trophozoites (34-37 hpi) were resuspended to 2 x 10^7 parasites/mL using the same method as previously described. Pluronic F-127 (Sigma-Aldrich, USA, 0.1 % v/v) and APG-1 (Abcam, UK, final concentration 5 µM) was added to the parasite suspension and incubated in

a stationary incubator (MRC LM-570 incubator, Israel) for 60 min at 37 °C in the dark. After 60 min of incubation, the samples were transferred to a 96 well plate and fluorescence was read using a Fluoroskan Ascent FL microplate fluorimeter (Thermo Scientific, USA; excitation 490 nm, emission 520 nm). Malaria saline with 0.025-0.2 % DMSO as required as vehicle control was used with Pluronic F-127 (0.1 % v/v) and APG-1 (final concentration 5 μM) as background fluorescence control. Excel was used to analyse the data where the background was subtracted, and the data was normalised relative to the untreated parasites.

To determine the ideal concentration of APG-1 to be used with this assay, parasites were isolated and resuspended to 2 x 10^7 parasites/mL. Different concentrations of APG-1 were tested at the same incubation time as shown in the table below. Subsequently, different incubation times were tested at a single concentration (Table 3.2)

Table 3.2: Conditions for optimal APG-1 fluorescence signal in isolated *P. falciparum* parasites.

	APG-1 concentration (μM)	**Incubation time (min)**
Optimal concentration	0.1	60
	5	
	10	
Optimal incubation time	5	10
		30
		60

To determine whether Paxilline can protect against K^+ loss from the parasite by blocking K^+ channels, the isolated parasites were resuspended in K^+ free malaria saline [125 mM NaCl, 5 mM Choline chloride (Glentham Life Sciences, UK), 25 mM HEPES, 20 mM Glucose, and 1 mM $MgCl_2$, pH 7.1], and normal malaria saline given above. Samples were incubated for 15 min with the drug before adding Pluronic F-127 (0.1 % v/v) and APG-1 (final concentration 5 μM). DMSO (0.1 % v/v) was included in the cell-free malaria saline to measure background fluorescence.

To determine the effect that different compounds have on intracellular K^+ levels, different experimental conditions were used as described above. Isolated trophozoites resuspended to 2 x 10^7 parasites/mL were incubated for 15 min with the compound(s) before APG-1 (final concentration 5 μM) and Pluronic F-127 (final concentration 0.1 % v/v) was added, the sample incubated for 60 min and fluorescence measured as described above.

3.6. Fluorescent imaging of $DiBAC_4(3)$ and APG-1 stained *P. falciparum* parasites

A majority trophozoite (95 %) parasite culture at ~ 8 % parasitaemia was centrifuged for 2 min at 3260 x*g* in a SL 8R centrifuge, the media aspirated and the pellet resuspended in 400 µL normal malaria saline. Subsequently, either $DiBAC_4(3)$ (final concentration 250 nM) or APG-1 (final concentration 5 µM) was added. Alternatively, the parasites were isolated from the erythrocytes using saponin (0.05 % v/v) and resuspend in 400 µL of malaria saline with either 250 nM $DIBAC_4(3)$ or 5 µM APG-1. Both infected erythrocytes and isolated parasites were incubated at 37 °C for 30 min ($DiBAC_4(3)$) or 60 min (APG-1) after which a 10 µL sample was seeded onto a slide and covered with a coverslip. Images were captured using an EVOS M5000 cell imaging system (oil immersion at 1 000x magnification), with excitation at 470 nm and emission at 525 nm. Images were processed using ImageJ version 1.54g.

4. Results

4.1. *In vitro* production of intraerythrocytic *P. falciparum* parasites

Asexual *P. falciparum* NF54, Dd2 and K1 parasites were cultured *in vitro* for the SYBR Green 1 proliferation assay while NF54 parasites were used for all other experiments. All developmental stages of the asexual parasite were observed during the 48 h life cycle (Figure 4.1). Ring-stage parasites were present at 1-16 hpi recognizable by the indented circle shape. Trophozoites were observed between 18 and 37 hpi, distinguishable by the increase in cytoplasm size and density along with the formation of the hemozoin crystal. The multinucleated schizont developed from 38-48 hpi after which it burst and released merozoites to invade new erythrocytes to restart the life cycle.

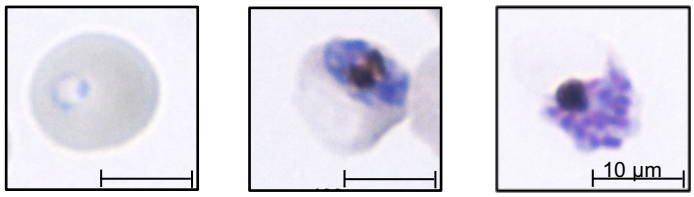

Figure 4.1: *P. falciparum* asexual lifecycle development. Asexual *P. falciparum* NF54 parasite development from ring stage to schizont stage over the 48 h life cycle. Parasites were visualized using a light microscope at 1000x magnification with RapiDiff stained slides.

4.2. Membrane potential dye $DiBAC_4(3)$ responds to Δψ in isolated *P. falciparum* parasites

$DiBAC_4(3)$ is a voltage sensitive fluorescent dye used to measure Δψ of cells (Yamada et al., 2001), where membrane depolarisation causes the electrostatic attraction of this anionic dye to the membrane, resulting in an increased signal. However, a hyperpolarised membrane potential reduces the electrostatic interaction of the dye with the membrane, causing a lower signal (Maher et al., 2007). The fluorescence of $DiBAC_4(3)$ was associated with the plasma membrane in infected erythrocytes, where concentrated staining can be observed for both the EPM and the PPM. In isolated parasites fluorescence was associated with PPM (Figure 4.2).

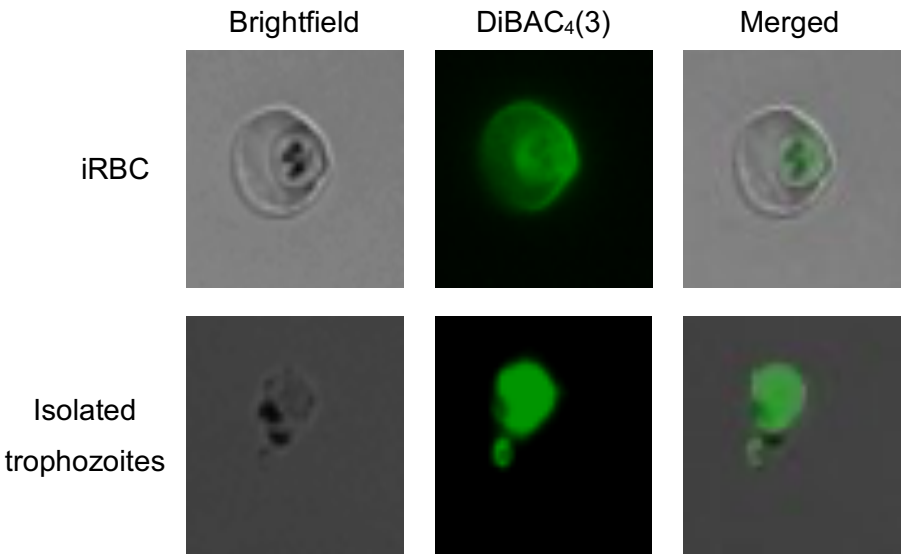

Figure 4.2: Localisation of the membrane potential sensitive fluorescent dye DiBAC$_4$(3) in isolated *P. falciparum* trophozoites. Localisation of DiBAC$_4$(3) in infected erythrocytes and isolated trophozoites, observed using the EVOS M5000 cell imaging system under 1 000x magnification (oil immersion), with excitation at 470 nm and emission at 525 nm. On the left panel is the brightfield image followed by the fluorescence image in the middle. The right panel is the superimposed image of the fluorescence image on to the brightfield image. Images were processed using ImageJ version 1.54g.

Previously uninfected erythrocytes was stained with 250 nM of the dye incubated for 30 min prior to any measurements (Moersdorf et al., 2013). By contrast, the single previous use of DiBAC$_4$(3) in isolated *P. falciparum* parasites used 1.5 nM of the dye with kinetic measurements for 20 min (Allen and Kirk, 2004). Here, we optimised the conditions for a non-kinetic endpoint assay. DiBAC$_4$(3) had a concentration-dependent increase in signal-to-background (S/B) fluorescence at concentrations between 1.5 and 24 nM (Figure 4.3 A). A higher concentration of DiBAC$_4$(3) resulted in an increased signal at 250 nM, with no statistically significant difference in S/B between 24 and 250 nM (P=0.66, n=3, unpaired student t-test). Therefore, all samples were incubated with 250 nM DiBAC$_4$(3) for future studies.

To determine whether a longer incubation time will result in an increase in DiBAC$_4$(3) fluorescence, the signal was compared after 30 , 60 and 90 min of incubation. Longer incubation resulted in a decrease in the fluorescence value (Figure 4.3 B). Therefore, all subsequent incubations with DiBAC$_4$(3) were performed for 30 min.

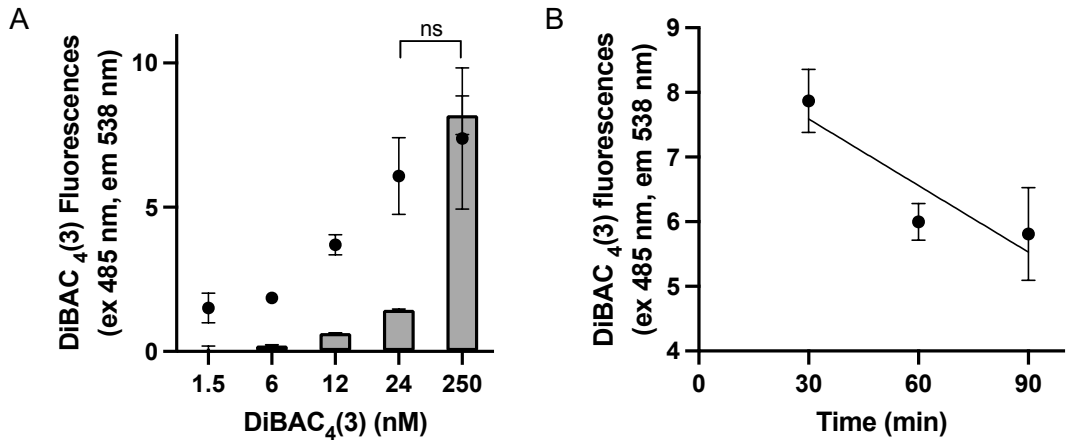

Figure 4.3: Optimization of DiBAC$_4$(3) fluorescence in isolated *P. falciparum* parasites. Isolated parasites were suspended in malaria saline at 3 x 10^7 parasites/mL and incubated with 250 nM DiBAC$_4$(3) for 30 min at 37 °C unless otherwise indicated. A) Fluorescence signal-minus-background (bars) and S/B ratios (symbols) at different dye concentrations. B) Fluorescence signals following different incubation times. Fluorescence was measured using a Fluoroscan Ascent FL microplate fluorometer, excitation at 485 nm and emission at 538 nm. Data are from n=3, each performed in technical triplicates with S.E.

A variety of different compounds with known biological effects were used to determine if DiBAC$_4$(3) responded as expected. Concanamycin A as a known V-type ATPase inhibitor induced depolarisation that led to a statistically significant increase in DiBAC$_4$(3) fluorescence (120 ± 10 % of control, n=6, $P \leq 0.05$, unpaired student t-test) (Figure 4.4 A). Likewise, membrane hyperpolarisation by ionophores that increase membrane permeability to either K^+ (Valinomycin) or both K^+ and Na^+ (Gramicidin) lead to a statistically significant decrease in DiBAC$_4$(3) fluorescence of 67 ± 9 % of control (n=3, P=0.04) and 86 ± 5 % of control (n=3, P=0.03 unpaired student t-test) respectively, due to the leak of K^+ out of the cell down the concentration gradient (Figure 4.4 A). While Nigericin (ionophore that increase membrane permeability to H^+ and K^+) also caused a decrease in DiBAC$_4$(3) fluorescence (90 ± 10 % of control, n=3, P=0.4, unpaired student t-test), this decrease was not statistically significant. Unexpectedly, Salinomycin (K^+ ionophore) did not have an effect on DiBAC$_4$(3) fluorescence under the test conditions.

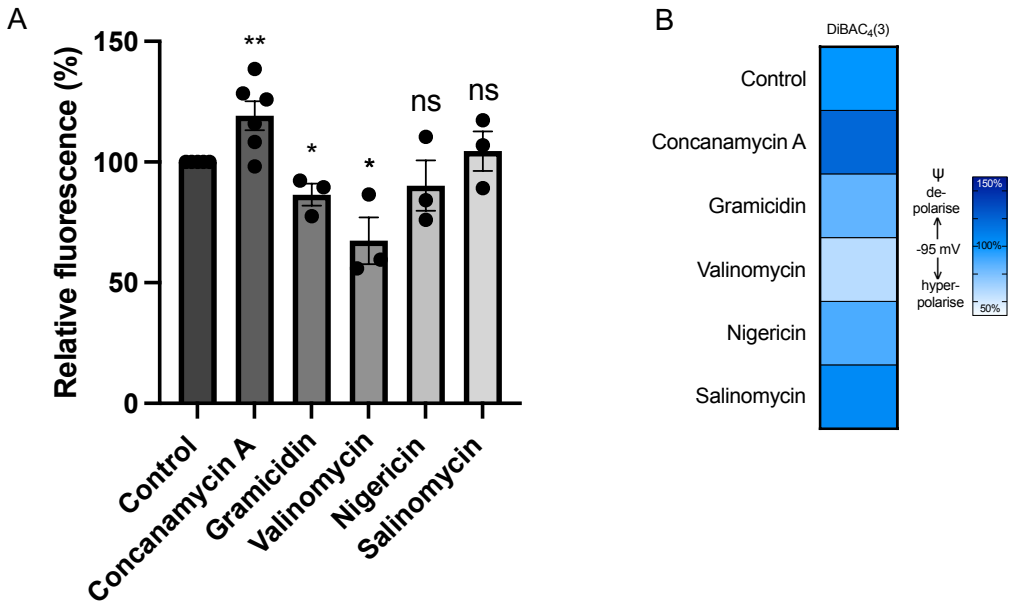

Figure 4.4: DiBAC$_4$(3) fluorescence respond to changes in Δψ and ion levels in isolated *P. falciparum* parasites. Isolated parasites were suspended in malaria saline at 3 x 10^7 parasites/mL and incubated with 250 nM DiBAC$_4$(3) for 30 min at 37 °C. A) Relative fluorescence following inhibition by Concanamycin A (200 nM), Gramicidin, Valinomycin, Nigericin, and Salinomycin (5 µM each). B) Heatmap representation of changes in DiBAC$_4$(3) fluorescent signal. Fluorescence was measured using a Fluoroscan Ascent FL microplate fluorometer, excitation at 485 nm and emission at 538 nm. Data are from n=3, each performed in technical triplicates with S.E., * =*P* <0.05, * * =*P* <0.01 unpaired student t-test compared to control.

The DiBAC$_4$(3) fluorescence assay was evaluated for the assay reproducibility (Z'-factor) and inner-assay reproducibility via % coefficient of variation (CV) (Zhang et al., 1999). The assay had an excellent Z'-factor of 0.87 (Iversen et al., 2006) and a low average % CV of 2.19 % (n=6). Therefore, DiBAC$_4$(3) fluorescence can be used to assess changes in the membrane potential of isolated *P. falciparum* parasites.

4.3. APG-1 responds to changes in K^+ in isolated *P. falciparum* parasites

Here, we investigated if we can use APG-1 to evaluate intracellular K^+ levels of isolated *P. falciparum* parasites. As expected, the fluorescence of APG-1 is localised to the parasite cytoplasm in both infected erythrocytes and isolated parasites, since K^+ levels of the infected erythrocyte cytosol are similar to the surrounding environment (Figure 4.5) (Kirk, 2015).

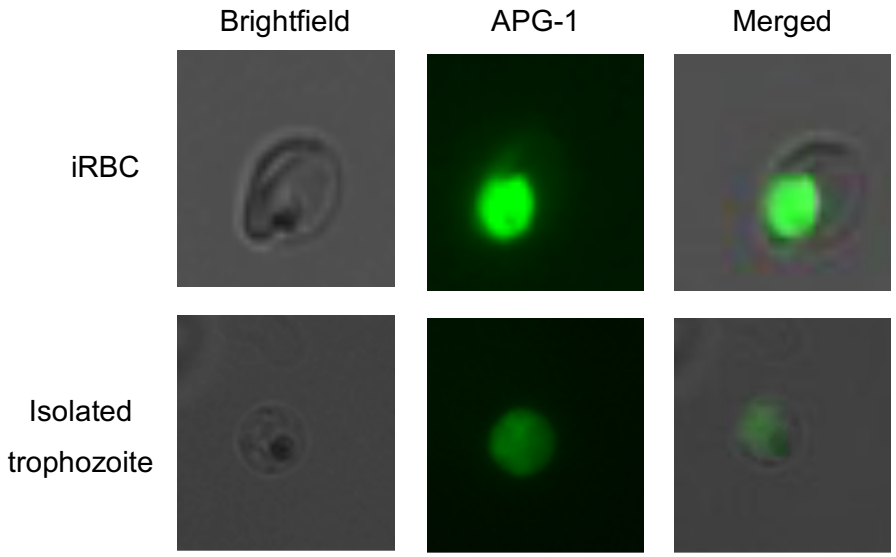

Figure 4.5: Localisation of the K^+ sensitive fluorescent dye APG-1 in *P. falciparum* trophozoites. Localisation of APG-1 in infected erythrocytes and isolated trophozoites, observed using the EVOS M5000 cell imaging system under 1 000x magnification (oil immersion), with excitation at 470 nm and emission at 525 nm. On the left panel is the brightfield image followed by the fluorescence image. The right panel is the superimposed image of the fluorescence image on to the brightfield image. Images were processed using ImageJ version 1.54g.

We evaluated the signal-minus-background and S/B measured for a range of APG-1 concentrations following a 60 min incubation, to allow for uptake and subsequent de-esterification of the dye. An increase in dye concentration from 1 to 5 µM did lead to an increase in signal-minus-background and S/B (from 0.07 to 0.90 and 1.14 to 6.34, respectively), although doubling the concentration to 10 µM did not increase the signal-minus-background (0.90 vs. 0.86) and led to a decrease in S/B (4.94 ± 0.19, n=3, unpaired student t-test) (Figure 4.6 A). APG-1 fluorescence increased over time from 10 to 60 min incubation. Given that the isolated parasites are no longer within the host erythrocyte, longer incubation times were not considered to ensure that >95 % of the parasites remain viable (Figure 4.6 B) (Saliba et al., 1998). Based on these results, all subsequent experiments used isolated *P. falciparum* parasites stained with 5 µM APG-1 for 60 min.

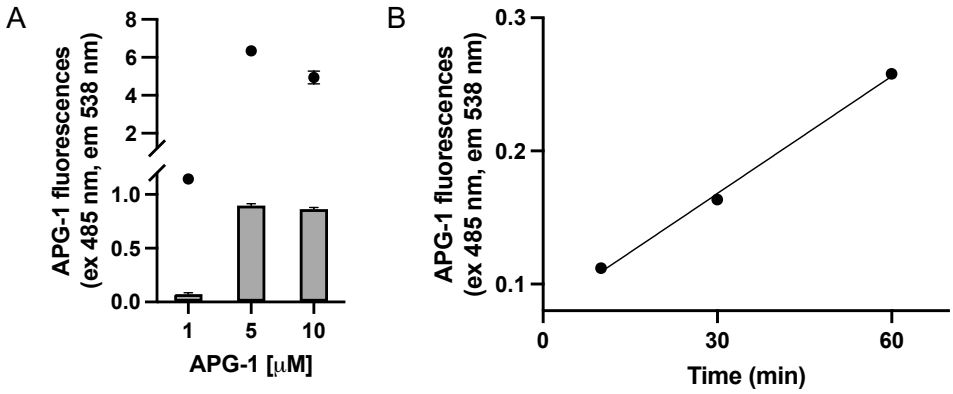

Figure 4.6: APG-1 fluorescence in isolated *P. falciparum* parasites. Isolated parasites were suspended in malaria saline at 2 x 10^7 parasites/mL. A) APG-1 fluorescent signal-minus-background (bars) and S/B ratios (symbols) incubated for 60 min at different dye concentrations. B) APG-1 (5 μM) signal response to different incubation time points. Fluorescence was measured using a Fluoroscan Ascent FL microplate fluorometer, excitation at 485 nm and emission at 538 nm. Data from n=1 in technical triplicate, shown with SD between technical triplicate.

Next, we evaluated if APG-1 fluorescence responds as expected to changes in Δψ and intracellular ion levels. PPM depolarisation induced by Concanamycin A (200 nM) inhibition of V-type ATPase leads to a statistically significant decrease in relative APG-1 fluorescence (63 ± 4 % of control, n=6, $P \leq 0.0001$, unpaired student t-test) (Figure 4.7 A) due to the decreased uptake of K^+ associated with the decreased Δψ. Similarly, treatment of isolated parasites with ionophores that increase membrane permeability to K^+ (Valinomycin and Salinomycin), K^+ and Na^+ (Gramicidin) or H^+ and K^+ (Nigericin) led to a statistically significant decrease in fluorescence due to the movement of K^+ out of the cell down the concentration gradient. Valinomycin (70 ± 6 % of control, n=3, P=0.007, unpaired student t-test), Nigericin (73 ± 4 % of control, n=3, P=0.003, unpaired student t-test), Gramicidin (61 ± 7 % of control, n=3, P=0.006, unpaired student t-test) and Salinomycin (66 ± 3 % of control, n=3, P=0.0006, unpaired student t-test) (Figure 4.7 B). No statistically significant difference was observed between the ionophores.

The assay had an excellent intra-assay variability with a Z'-factor of 0.84 (Iversen et al., 2006) and had a % CV of 3.59 % (n=6). Therefore, APG-1 fluorescence can be used to evaluate changes in cytosolic K^+ in isolated *P. falciparum* parasites.

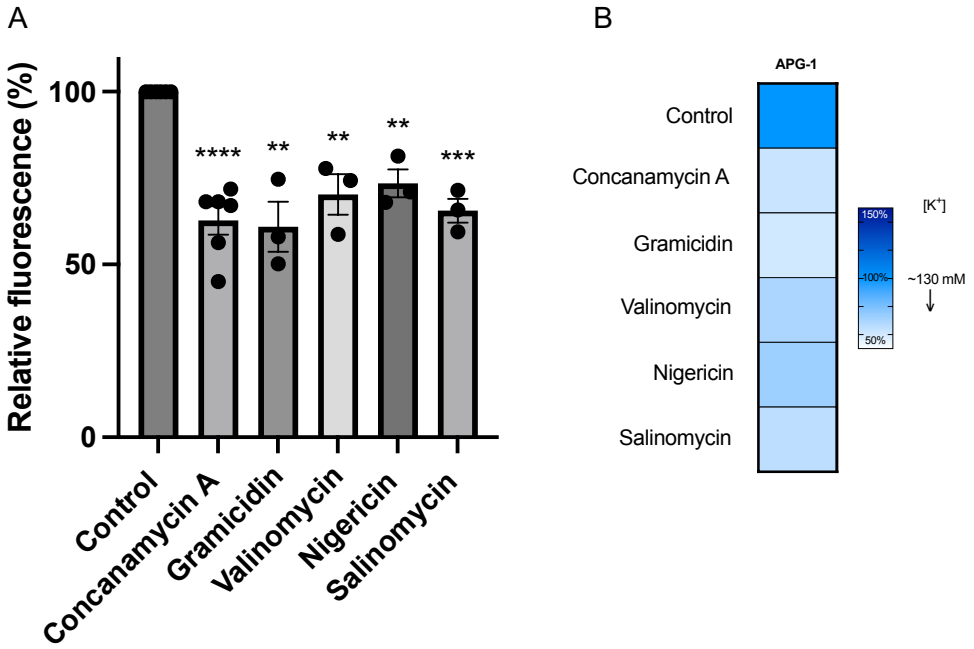

Figure 4.7: APG-1 fluorescence respond to changes in ion levels in isolated *P. falciparum* parasitesIsolated parasites were suspended in malaria saline at 2 x 10^7 parasites/mL, and stained with 5 µM APG-1 for 60 min 37 °C. A) APG-1 fluorescence values following inhibition by Concanamycin A (200 nM), Valinomycin, Nigericin, Gramicidin and Salinomycin (5 µM). B) Heatmap representation of changes in APG-1 fluorescent signal. Fluorescence was measured using a Fluoroscan Ascent FL microplate fluorometer, excitation at 485 nm and emission at 538 nm. Data from n≥3, each performed in technical triplicates with S.E., * * =*P* <0.01, * * * =*P* <0.001, * * * * =*P* <0.0001 unpaired student t-test compared to control.

4.4. Paxilline can be used as a control inhibitor of K^+ channels in isolated *P. falciparum* parasites

4.4.1. K^+ channel inhibitor selection process

A known V-type ATPase inhibitor was used above to validate the response of the $DiBAC_4(3)$ and APG-1 assays. At the start of the study a control compound with activity against *P. falciparum* parasites that specifically targets K^+ channels was not available. Therefore, several inhibitors with proven K^+ channel inhibition in other organisms were investigated for their activity against *P. falciparum* parasites.

127 compounds were identified from TargetMol (https://www.targetmol.com/target/Potassium_Channel/2) as known K^+ channel inhibitors in humans, mice and rats, amongst others (Figure 4.8). From these, 57 compounds blocked only K^+ channels, of which only 11 were specific for either Kv (6) or BK (5) K^+ channels. Compounds with a molecular weight greater than 500 g/mol were excluded to ensure that only drug-like compounds were tested. This resulted in the 6

compounds (AUT1, GAL-021, Paxilline, XE_991, 3,4-diaminopyridine and 4-aminopyridine) evaluated here.

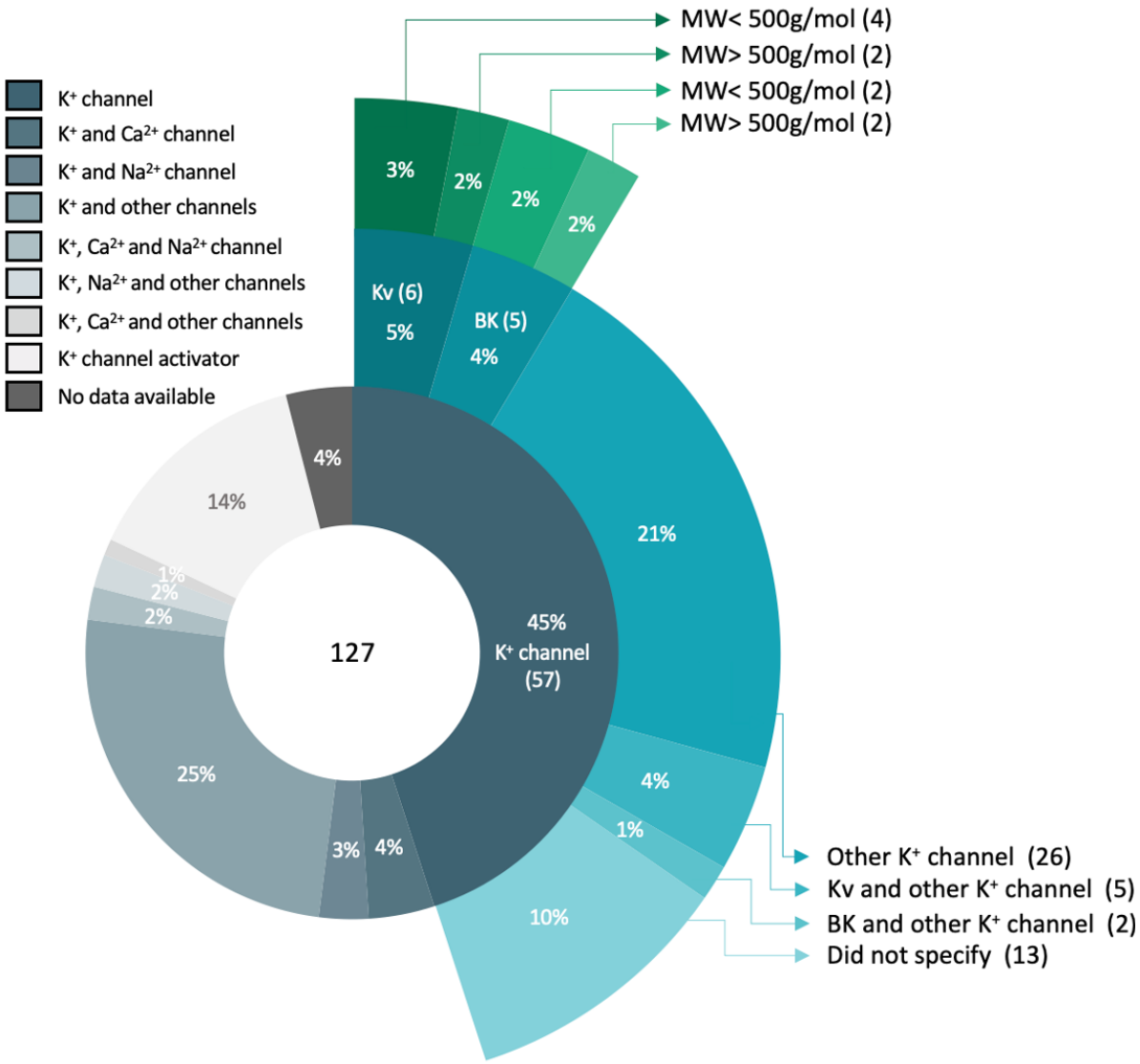

Figure 4.8: K^+ channel inhibitor selection process. The final 6 K^+ inhibitors were chosen from the initial 127 potential K^+ channel inhibitors. Inhibitors that were not specific to K^+ channels was removed first. From the 57 remaining inhibitors 11 was specific to either Kv or BK channels, of which only the final 6 had a molecular weight below 500 g/mol.

The six putative K^+ channel inhibitors were evaluated for their ability to affect asexual *P. falciparum* NF54 parasite proliferation (Figure 4.9). Of these, the fungal alkaloid Paxilline (a BK channel inhibitor) inhibited parasite proliferation in the low micromolar range (4.52 ± 0.23 µM) (Figure 4.9 A). Compared to Paxilline, the other identified BK channel inhibitor, AUT1, had a much lower effect on parasite proliferation, with an IC_{50} value of 84.6 ± 5.6 µM (Figure 4.9 B). The Kv channel inhibitors, XE_991 (IC_{50} of 36.16 ± 0.78 µM, Figure 4.9 C) and GAL_021 (86 ± 14 µM) (Figure 4.9 D), were also poorly active. Surprisingly, the standard K^+ channel inhibitors 4-aminopyridine (Figure 4.9 E) and 3,4-diaminopyridine (Figure 4.9 F) (Khammy et al., 2018, Maddison and Newsom-Davis, 2003) were in effect unable to prevent parasite

proliferation to any appreciable level with an IC_{50} of 350 ± 29 µM and 426.333 ± 0.001 µM, respectively.

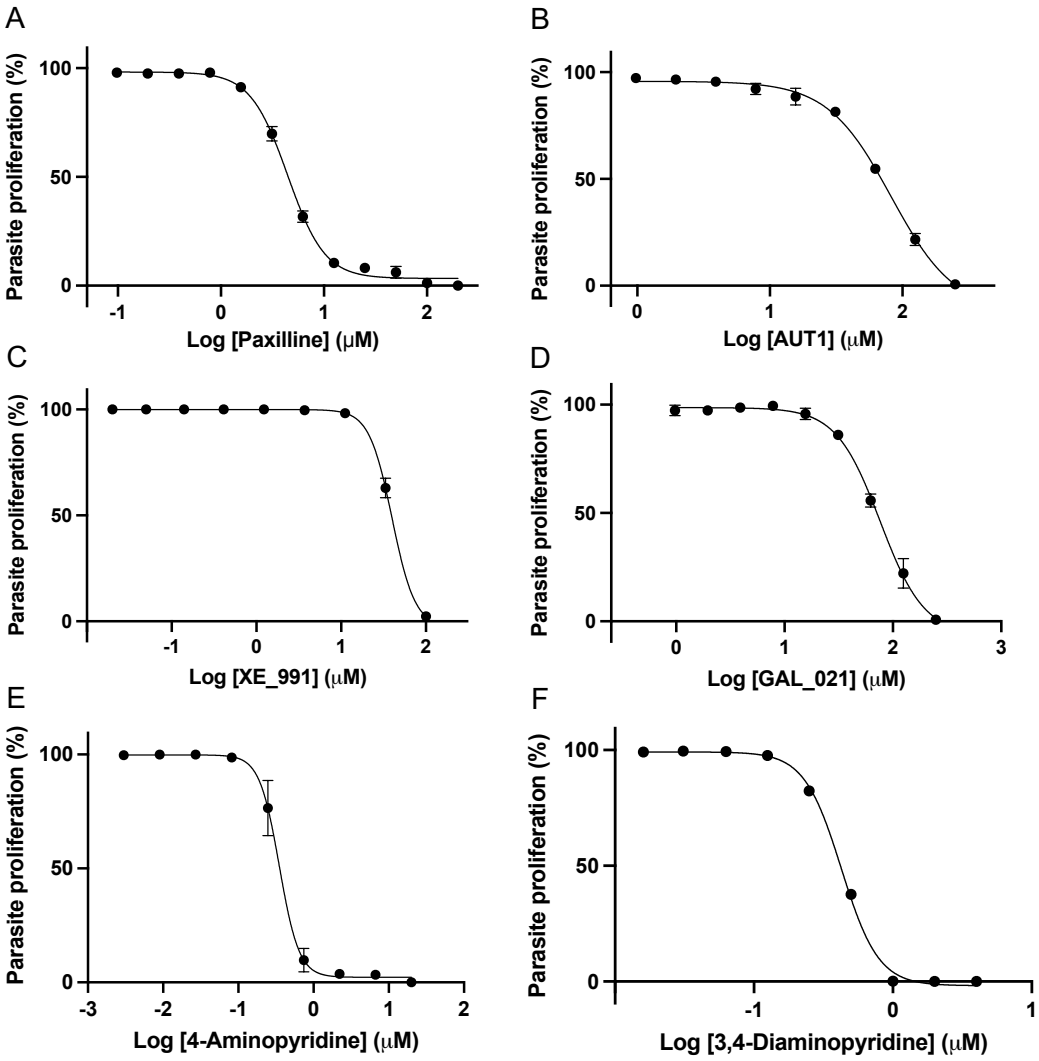

Figure 4.9: *In vitro* activity of K^+ channel inhibitors against the proliferation of asexual *P. falciparum* NF54 parasites. Inhibition of parasite proliferation by K^+ channel inhibitors was tested on synchronized*in vitro* intraerythrocytic *P. falciparum* NF54 parasites (1 % parasitaemia, 1 % haematocrit) and incubated for 96 h at 37 °C. A) Paxilline, B) AUT1, C) XE_991, D) GAL_021, E) 4-aminopyridine and F) 3,4-diaminopyridine. Data from n=3, each performed in technical triplicates with S.E. Where the error bars are not visible it falls within the symbol.

Based on the activity of Paxilline against drug-sensitive NF54 *P. falciparum* parasites, its activity against Dd2 (chloroquine resistant) and K1 (multidrug resistant) *P. falciparum* parasites were evaluated. Paxilline showed some gain in activity against these strains, with 67 ± 5 % and 71 ± 5 % inhibition against Dd2 and K1, when these parasites were treated with Paxilline at the NF54 IC_{50} concentration (4.5 µM) (Figure 4.10).

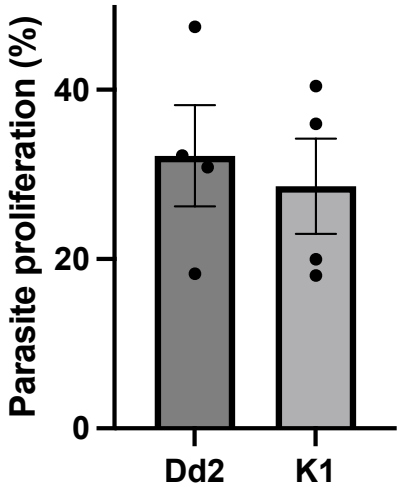

Figure 4.10: *In vitro* activity of Paxilline against the proliferation of drug-resistant *P. falciparum* strains. Synchronized *in vitro* intraerythrocytic *P. falciparum* Dd2 and K1 parasites (1 % parasitaemia, 1 % haematocrit) treatment with Paxilline (4.5 µM) and incubated for 96 h at 37 °C. Data from n=4, each performed in technical triplicates showing S.E.

4.4.2. Changes in $DiBAC_4(3)$ and APG-1 fluorescence confirm that Paxilline inhibits K^+ transport

To establish whether Paxilline can be used as a control K^+ channel inhibitor in both $\Delta\psi$ and K^+ level assays, both $DiBAC_4(3)$ and APG-1 fluorescence were measured following treatment of isolated *P. falciparum* parasites with different concentrations of Paxilline. $DiBAC_4(3)$ and APG-1 fluorescence showed a dose-dependent decrease in the presence of Paxilline (Figure 4.11), consistent with membrane hyperpolarisation due to decreased K^+ uptake via increased blocking of K^+ channels.

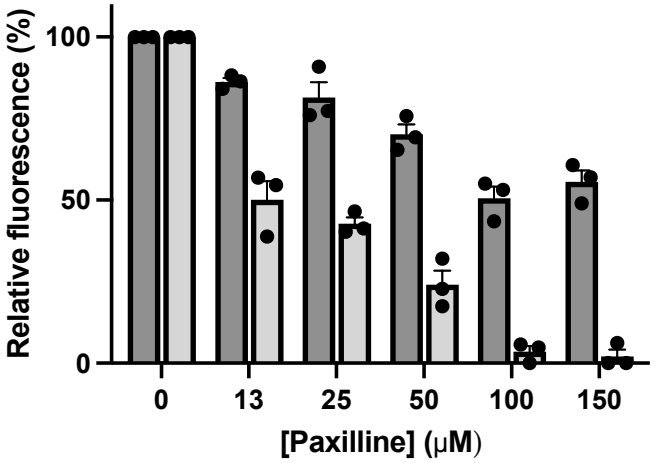

Figure 4.11: Paxilline has a dose-dependent effect on $DiBAC_4(3)$ and APG-1 fluorescence in isolated *P. falciparum* parasites. Isolated parasites were suspended in malaria saline and treated for 15 min at 37 °C with different concentrations of Paxilline prior to staining: 3 x 10^7 parasites/mL incubated with 250 nM $DiBAC_4(3)$ for 30 min (dark grey) or 2 x 10^7 parasites/mL stained with 5 µM APG-1 for 60 min (light grey). Fluorescence was measured using a Fluoroscan Ascent FL microplate fluorometer, excitation at 485 nm and emission at 538 nm. Data from n=3, each performed in technical triplicates with S.E.

Furthermore, Paxilline non-significantly decreased the loss of APG-1 fluorescence observed when the outward K^+ concentration gradient is increased by removing external K^+ (Figure 4.12). These results confirm that Paxillin inhibits K^+ channels and can be used as a control compound in both assays.

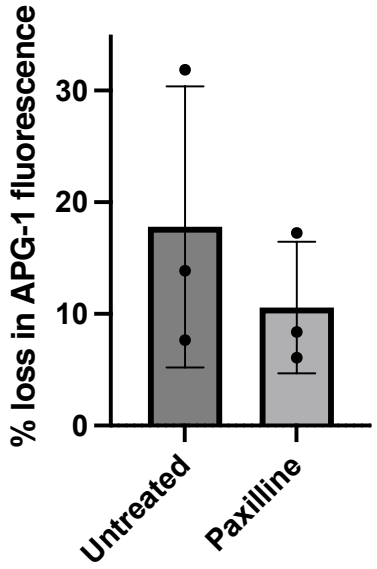

Figure 4.12: Paxilline has a protective effect against loss of APG-1 fluorescence in the absence of external K^+. Isolated parasites were suspended in normal malaria saline and K^+ free malaria saline at 2 x 10^7 parasites/mL and stained with 5 µM APG-1 for 60 min at 37 °C in the presence or absence of Paxilline (50 µM). Fluorescence was measured using a Fluoroscan Ascent FL microplate fluorometer, excitation at 485 nm and emission at 538 nm. Data from n=3, each performed in technical triplicates with S.E.

4.5. Evaluation of changes in the Δψ and intracellular K^+ levels in isolated *P. falciparum* parasites following compound treatment

4.5.1. $DiBAC_4(3)$ and APG-1 confirms changes in K^+ levels following treatment with previously predicted K^+ channel inhibitors

Previously, the antiproliferative effects of some compounds were ascribed to inhibition of K^+ channels (Table 1.1) (Waller et al., 2008a). Here, we evaluated if these compounds result in membrane hyperpolarisation (decrease in $DiBAC_4(3)$ fluorescence) and reduced K^+ levels, as expected from K^+ channel inhibitors (Figure 4.13 A). The bee toxin Apamine did not change $DiBAC_4(3)$ and APG-1 fluorescence, consistent with the lack of inhibitory effect on parasite proliferation previously observed (Waller et al., 2008a). Quinine had no statistically significant effect on the $DiBAC_4(3)$ fluorescence. In contrast, Quinine resulted in a statistically significant decrease in APG-1 fluorescence (89 ± 1 % of control, n=3, P=0.04, unpaired student t-test). Parasites treated with Tubocurarine chloride showed an unexpected statistically significant increase in $DiBAC_4(3)$ fluorescence (105 ± 7 % of control, n=3, P=0.007, unpaired student t-

test) and a statistically significant decrease in APG-1 fluorescence (90 ± 2 % of control, n=3, *P*=0.005, unpaired student t-test). These results support previous postulations that inhibition of the K^+ channel is at least partially responsible for the observed proliferation inhibition seen with Quinine and Tubocurarine chloride (Waller et al., 2008a).

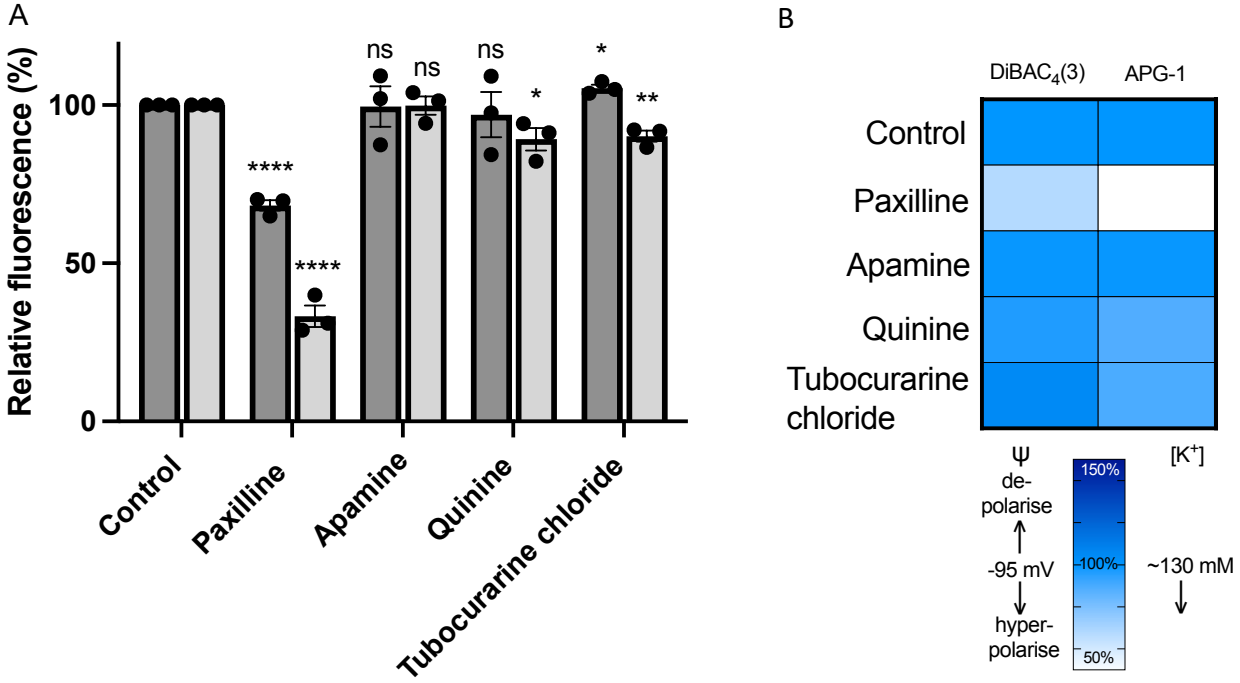

Figure 4.13: $DiBAC_4(3)$ and APG-1 fluorescence following treatment with putative K^+ channel inhibitors previously used in *Plasmodium*. Isolated parasites were suspended in malaria saline and treated for 15 min at 37 °C with Apamine (10 µM), Quinine (10 µM), and Tubocurarine chloride (10 µM) prior to staining: 3 x 10^7 parasites/mL incubated with 250 nM $DiBAC_4(3)$ for 30 min (dark grey), or 2 x 10^7 parasites/mL stained with 5 µM APG-1 for 60 min (light grey). Paxilline (50 µM) was added as a K^+ channel inhibitor control. B) Heatmap representation of changes in fluorescent signal. Fluorescence was measured using a Fluoroscan Ascent FL microplate fluorometer, excitation at 485 nm and emission at 538 nm. Data from n=3, each performed in technical triplicates with S.E., * =*P* <0.05, * * =*P* <0.01, * * * * =*P* <0.0001, unpaired student t-test compared to control.

4.5.2. No difference observed in $DiBAC_4(3)$ and APG-1 fluorescence following treatment with antimalarials with known MoA

$DiBAC_4(3)$ and APG-1 fluorescent assays were tested using antimalarial compounds with known MoA to ensure that no non-specific changes are detected. Chloroquine (inhibits the conversion of haem to haemozoin), Dihydroartemisinin (inhibits haem detoxification), Pyrimethamine (targets dihydrofolate reductase) and Sulfadoxine (targets dihydropteroate synthase and dihydrofolate reductase) was chosen since their MoA should not affect Δψ or intracellular K^+ levels. No change in $DiBAC_4(3)$ or APG-1 fluorescence was observed for these antimalarials (Figure 4.14). These results confirm that $DiBAC_4(3)$ fluorescence changes are due to changes in membrane potential, and APG-1 fluorescence changes are due to changes in K^+ levels and not to general drug-induced cellular stress.

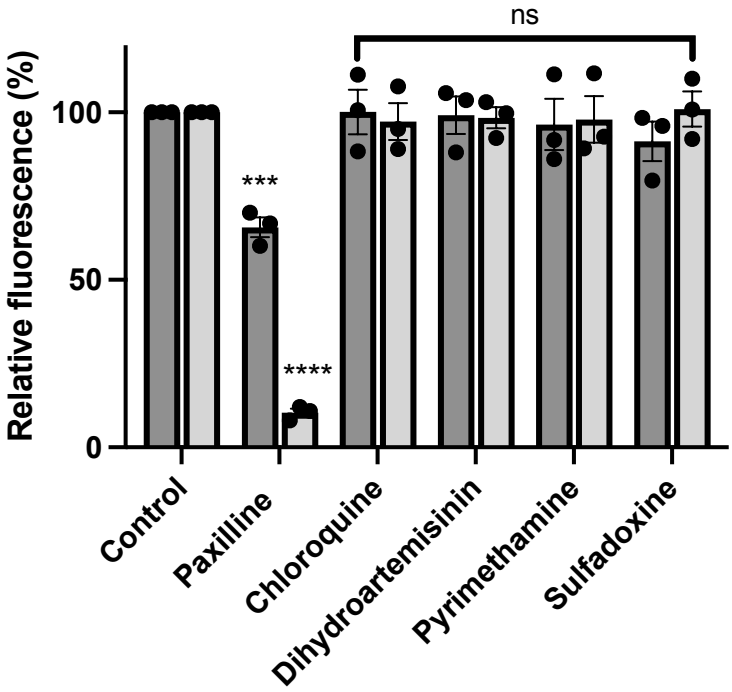

Figure 4.14: DiBAC$_4$(3) and APG-1 fluorescence in isolated *P. falciparum* parasites treated with antimalarials with known MoA. Isolated parasites were suspended in malaria saline and treated for 15 min at 37 °C with Chloroquine (10 µM), Dihydroartemisinin (10 µM), Pyrimethamine (10 µM), and Sulfadoxine (10 µM) before dye was added: 3 x 10^7 parasites/mL incubated with 250 nM DiBAC$_4$(3) for 30 min (dark grey) or 2 x 10^7 parasites/mL with 5 µM APG-1 for 60 min (light grey). Paxilline (50 µM) was added as a K^+ channel inhibitor control. Fluorescence was measured using a Fluoroscan Ascent FL microplate fluorometer, excitation at 485 nm and emission at 538 nm. Data from n=3, each performed in technical triplicates with S.E., * * * =*P* <0.001, * * * * =*P* <0.0001, unpaired student t-test compared to control.

4.5.3. The effect of ion maintenance inhibitors on DiBAC$_4$(3) and APG-1 fluorescence signal in isolated *P. falciparum*

Next, we investigated whether the inhibition of ion maintenance targets have distinct profiles measurable with DiBAC$_4$(3) and APG-1. Inhibition of V-type ATPase leads to less H^+ being exported, the membrane becoming depolarised, and less K^+ being able to enter the cell. This can be seen by the statistically significant increase in DiBAC$_4$(3) fluorescence, (128 ± 6 % of control, n=3, *P*=0.01, unpaired student t-test, Figure 4.15, dark grey) in Concanamycin A treated parasites. The significant decrease in APG-1 fluorescence signal (57 ± 7 % of control, n=3, *P*=0.0006, unpaired student t-test, light grey) indicate K^+ import decreasing due to the membrane depolarising. Inhibition of PfATP4 results in less H^+ being imported and leads to the membrane hyperpolarising due to H^+ still being exported by the V-type ATPase. In the presence of KAE609 there was no statistically significant effect on DiBAC$_4$(3) fluorescence (114 ± 11 % of control, n=3, unpaired student t-test). Likewise, there was no difference in APG-1 fluorescence,(102 ± 1 % of control, n=3, unpaired student t-test) indicating no change in intracellular K^+ levels. The inhibition of K^+ channels results in the halt of K^+ influx into the cell,

consequently leading to membrane hyperpolarisation. This was observed by the highly statistically significant decrease of both $DiBAC_4(3)$ and APG-1 fluorescence (52 ± 9 % of control, n=3 *P*=0.006 and 33 ± 3 % of control, n=3 *P*<0.0001, unpaired student t-test).

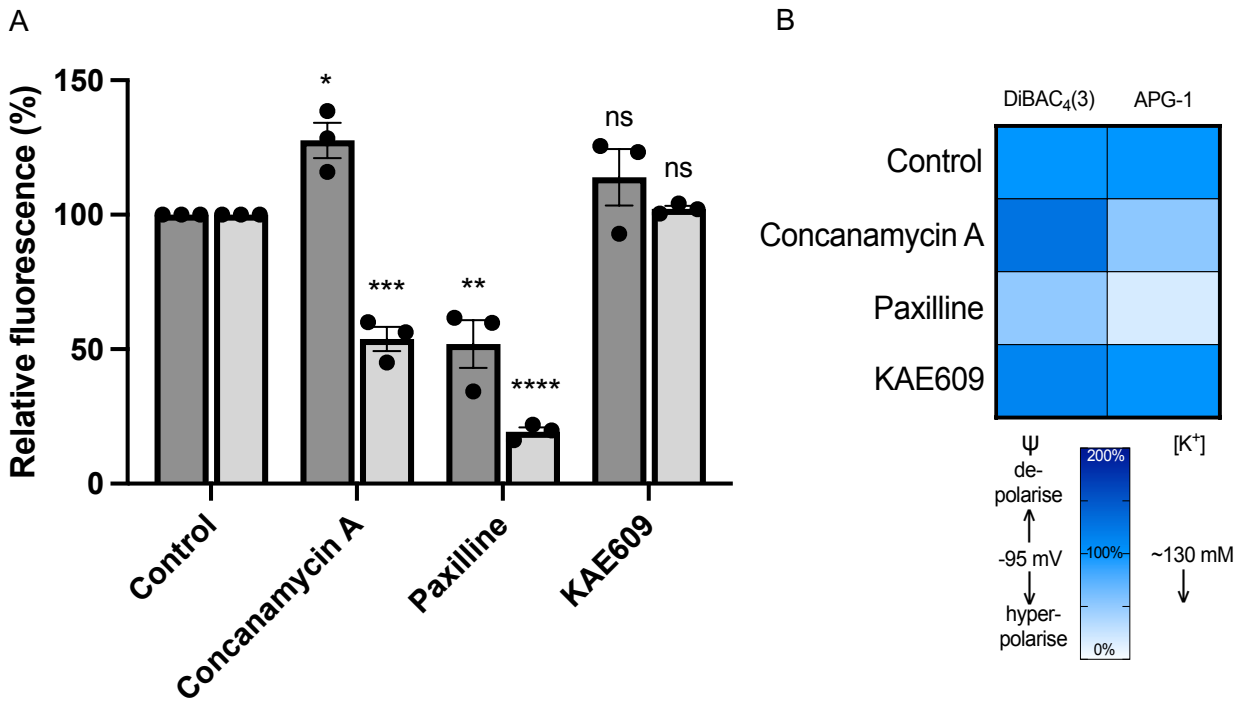

Figure 4.15: $DiBAC_4(3)$ and APG-1 fluorescence in isolated *P. falciparum* parasites subsequent to ion maintenance inhibition. Isolated parasites were suspended in malaria saline and treated for 15 min at 37 °C with either Concanamycin A (200 nM), Paxilline (50 µM), KAE609 (1 µM) before dye was added: 3 x 10^7 parasites/mL incubated with 250 nM $DiBAC_4(3)$ for 30 min (dark grey) or 2 x 10^7 parasites/mL with 5 µM APG-1 for 60 min (light grey). B) Heatmap representation of changes in fluorescent signal. Fluorescence was measured using a Fluoroscan Ascent FL microplate fluorometer, excitation at 485 nm and emission at 538 nm. Data from n=3, each performed in technical triplicates with S.E., * =*P* <0.05, * * =*P* <0.01, * * * =*P* <0.001, * * * * =*P* <0.0001, unpaired student t-test compared to control.

4.5.4. The use of $DiBAC_4(3)$ and APG-1 to identify the mechanism of action of new compounds

Screening of the Medicines for Malaria Venture (MMV) Pandemic Response Box identified hits with similarity to ion channel inhibitors (Reader et al., 2021), Clemizole and MMV1634391. To evaluate if the antiproliferative effects of these compounds are due to interference with ion maintenance, we tested the effect on Δψ and K^+ levels. Clemizole had a slight, non-statistically significant decrease in $DiBAC_4(3)$ fluorescence with no change in APG-1 fluorescence observed. MMV1634391 showed a statistically significant, but slight decrease in both $DiBAC_4(3)$ fluorescence (92 ± 2 % of control, n=3, *P*=0.02, unpaired student t-test) and APG-1 fluorescence (90 ± 5 % of control, n=3, *P*=0.03, unpaired student t-test) (Figure 18).

Therefore, MMV1634391 affects both Δψ and intracellular K^+ levels, which may contribute to the antiplasmodial effect of this compound.

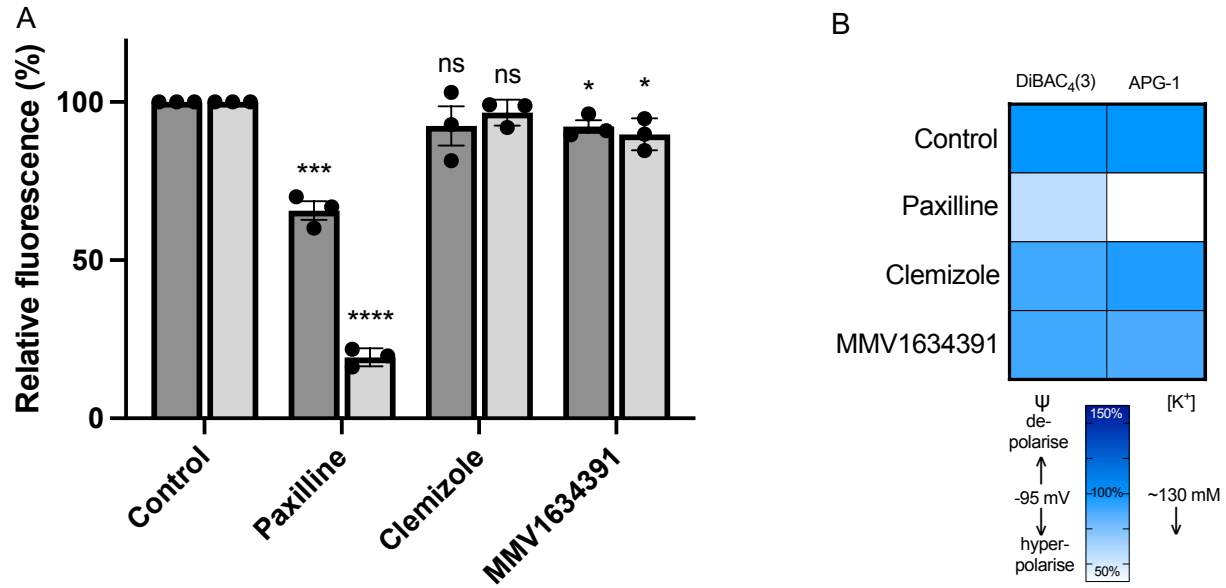

Figure 4.16: $DiBAC_4(3)$ and APG-1 as a tool to identify the mode of action of new compounds. Isolated parasites were suspended in malaria saline and treated for 15 min at 37 °C with either Clemizole (10 µM) or MMV1634391 (10 µM) before the respective dye was added: 3 x 10^7 parasites/mL incubated with 250 nM $DiBAC_4(3)$ for 30 min (dark grey) or 2 x 10^7 parasites/mL with 5 µM APG-1 for 60 min (light grey). Paxilline (50 µM) was added as a K^+ channel inhibitor control. B) Heatmap representation of changes in fluorescent signal. Fluorescence was measured using a Fluoroscan Ascent FL microplate fluorometer, excitation at 485 nm and emission at 538 nm. Data from n=3, each performed in technical triplicates with S.E.* =*P* <0.05, * * =*P* <0.01, * * * =*P* <0.001, * * * * =*P* <0.0001, unpaired student t-test compared to control.

5. Discussion

There are two broad strategies for screening antimalarial compounds: whole-cell phenotypic assays or target-specific assays. Whole-cell phenotypic assays first evaluate the effect of compounds on parasite survival. This is followed by the identification of the target (Armstrong et al., 2023), or at a minimum, investigation of the MoA of the compound using, for example, transcriptomics, metabolomics (Niemand et al., 2021, Birkholtz et al., 2008, van der Watt et al., 2018, Allman et al., 2016) whole-genome analysis, and/or *in silico* approaches. These are all extensive and time-consuming strategies with limited throughput. Alternatively, if a discrete target is known, a target-specific assay can be established to identify compounds that specifically interact with the target, with the effect on parasite survival only investigated later (Armstrong et al., 2023). For example, a *Plasmodium* Kinase Enzymology Platform has been established (Arendse et al., 2021, Cheuka et al., 2021), as well as an Arf GTPase assays for the discovery of antiplasmodial compounds that target specific biological functions (Swart et al., 2020).

Ion homeostasis is an essential biological function within the *P. falciparum* parasite. Prior to erythrocyte invasion, a non-infected erythrocyte maintains a low Na^+/high K^+ environment, however, an infected erythrocyte deviates from this and maintains a high Na^+/low K^+ environment as a consequence of NPP production in trophozoites (Mauritz et al., 2011, Kirk, 2015). A crucial factor in maintaining membrane potential is the presence of ion channels such as the V-type ATPase, PfATP4 and K^+ channels. Previous studies have shown that the inhibition of the V-type ATPase and PfATP4 leads to parasite death (Hayashi et al., 2000, Krishna et al., 2001), with additional inhibitory compounds identified using assays that measure the characteristic biological effect these compounds have (Lehane et al., 2014). Furthermore, similarly disrupting the K^+ concentration in the parasite through inhibition with compounds or ionophores leads to parasite death (D'Alessandro et al., 2015). However, these studies did not correlate the death response to intracellular K^+ levels. Therefore, in this study we developed an assay platform capable of measuring changes in membrane potential and intracellular K^+ levels using fluorescent dyes.

As the fluorescence obtained by using infected erythrocytes would not be a true indication of changes in membrane potential or intracellular K^+ levels of parasites, the parasites were isolated from the erythrocyte. $DiBAC_4(3)$ and APG-1 were both able to detect changes in $\Delta\psi$ and intracellular K^+ levels by using the V-type ATPase specific inhibitor Concannamycin A, which has a direct effect on $\Delta\psi$ and intracellular K^+ levels (van Schalkwyk et al., 2010). $DiBAC_4(3)$ and APG-1 are shown to be sensitive to $\Delta\psi$ and intracellular K^+ levels, respectively, and the changes in fluorescence obtained in other experiments are not due to a general death

response. $DiBAC_4(3)$ and APG-1 additionally respond to parasites treated Paxilline, a BK specific channel inhibitor (Zhou et al., 2020), as expected. This also supports previous work done on *P. falciparum* K^+ channels that indicated the possibility of parasites having BK channels with corresponding homologous regions (Waller et al., 2008b). Previous studies have shown that the disruption of K^+ homeostasis via ionophores is detrimental to *P. falciparum* asexual parasites although the direct effect on K^+ levels was not tested (D'Alessandro et al., 2015). In this study we confirmed that the death response previous studies reported was in fact due to disruption of K^+ homeostasis. In another study, the direct effect various K^+ channel inhibitors had on *P. falciparum* proliferation did not explore the effect these inhibitors had on K^+ levels (Waller et al., 2008a). Here we tested three of the inhibitors and confirmed that two inhibitors, namely Quinine and Tubocurarine chloride, had a significant effect on intracellular K^+ levels. In contrast, Apamine had no effect on intracellular K^+ levels, as expected since an IC_{50} value could not be obtained for this inhibitor. It is unclear whether this is due to the molecular weight of this compound or its low transport capability.

By taking a closer look at three ion maintenance targets, namely PfATP4, V-Type-ATPase and K^+ channels, we set out to identify discrete profiles to differentiate between the target inhibition by using the combination of $DiBAC_4(3)$ and APG-1 results. Out of the three targets, distinct profiles could only be obtained for V-type ATPase and K^+ channel inhibition. V-type ATPase inhibition led to an increase in $DiBAC_4(3)$ fluorescence and a decrease APG-1 fluorescence, whereas K^+ channel inhibition led to a decrease in both fluorescent dyes. PfATP4 inhibition led to a slight increase in $DiBAC_4(3)$ fluorescence, and no change was detected in APG-1 fluorescence. Therefore, both dyes need to be used to distinguish between V-type ATPase inhibition and K^+ channel inhibition. Two compounds with predicted general ion channel inhibition were used as test compounds to determine whether $DiBAC_4(3)$ and APG-1 can identify the possible target using the two discrete profiles. Although both compounds had a decrease in fluorescence, only MMV1634391 had a significant decrease in both $DiBAC_4(3)$ and APG-1 fluorescence, indicating that this compound could possibly be a K^+ channel inhibitor.

In addition to determining a compounds mode of action in the parasite, this assay can also provide critical information for the human host. The human cardiac K^+ channel encoded by human ether-à-go-go related gene (hERG) is involved in the cardiac repolarisation following cardiac action potential (Garrido et al., 2020). Compounds that block cardiac K^+ channels result in long QT intervals that can induce lethal ventricular tachyarrhythmias (Garrido et al., 2020). The inhibition of hERG can be measured using electrophysiological examinations of stably expressed recombinant channels or isolated cardiac myocytes (Priest et al., 2008). However, these technologies are low-throughput and labour intensive and are thus typically performed

later in the drug discovery process. We propose that compounds that show changes in *P. falciparum* intracellular K^+ levels using our assay should be earmarked for early hERG investigations.

APG-1 has successfully been utilized in other cell types but has never been applied in *Plasmodium* (Rana et al., 2019, Rimmele and Chatton, 2014). Here, we show that APG-1 can successfully be used to detect changes in intracellular K^+ levels in *P. falciparum*. In future studies, these assay platforms can be used collectively to determine the mode of action of compounds with unknown targets. Additionally, $DiBAC_4(3)$ and APG-1 can be calibrated to quantitatively determine $\Delta\psi$ and intracellular K^+ levels in the parasite. Thus, these assays hold promise to investigate gametocyte $\Delta\psi$ and K^+ levels.

6. Conclusion

Malaria remains one of the most important parasitic diseases, plaguing the African continent. It is therefore essential to identify novel drug targets for the development of chemotherapeutics that target unexplored biological processes. *P. falciparum* relies on K^+ import to maintain a - 95 mV membrane potential. Hence, perturbation of this process compromises parasite proliferation. Here, we established fluorescent assays to investigate membrane potential and steady-state intracellular K^+ levels.

This project aimed to establish fluorescent assays to detect changes in membrane potential and intracellular K^+ levels in *P. falciparum* asexual parasites. Here we established a fluorescent assay utilizing APG-1 to measure intracellular K^+ levels and showed that K^+ channel inhibition correlates to a decrease in intracellular K^+ levels. Additionally, $DiBAC_4(3)$ was used as proxy for membrane potential and could indicate membrane depolarisation when inhibiting the V-Type-ATPase. K^+ channel inhibition leads to membrane hyperpolarisation as expected when treated with a K^+ channel inhibitor identified through *in silico* studies. Furthermore, these fluorescent assay results show distinct profiles between V-Type-ATPase and K^+ channel inhibition. This supports the use of these dyes as preliminary mode of action indicators to distinguish between V-Type-ATPase and K^+ channel inhibition. Future studies may explore the calibration of APG-1 to determine exact K^+ levels in gametocytes.

References

ADOVELANDE, J. & SCHREVEL, J. 1996. Carboxylic ionophores in malaria chemotherapy: the effects of monensin and nigericin on *Plasmodium falciparum in vitro* and *Plasmodium vinckei petteri in vivo*. *Life Sci,* 59**,** PL309-15.

AHMAD, S. S., RAHI, M., RANJAN, V. & SHARMA, A. 2021. Mefloquine as a prophylaxis for malaria needs to be revisited. *Int J Parasitol Drugs Drug Resist,* 17**,** 23-26.

ALLEN, R. J. & KIRK, K. 2004. The membrane potential of the intraerythrocytic malaria parasite *Plasmodium falciparum*. *J Biol Chem,* 279**,** 11264-72.

ALLMAN, E. L., PAINTER, H. J., SAMRA, J., CARRASQUILLA, M. & LLINAS, M. 2016. Metabolomic Profiling of the Malaria Box Reveals Antimalarial Target Pathways. *Antimicrob Agents Chemother,* 60**,** 6635-6649.

ANTO, F., AGONGO, I. H., ASOALA, V., AWINI, E. & ODURO, A. R. 2019. Intermittent Preventive Treatment of Malaria in Pregnancy: Assessment of the Sulfadoxine-Pyrimethamine Three-Dose Policy on Birth Outcomes in Rural Northern Ghana. *J Trop Med,* 2019**,** 6712685.

ARENDSE, L. B., WYLLIE, S., CHIBALE, K. & GILBERT, I. H. 2021. *Plasmodium* Kinases as Potential Drug Targets for Malaria: Challenges and Opportunities. *ACS Infect Dis,* 7**,** 518-534.

ARMSTRONG, J. F., CAMPO, B., ALEXANDER, S. P. H., ARENDSE, L. B., CHENG, X., DAVENPORT, A. P., FACCENDA, E., FIDOCK, D. A., GODINEZ-MACIAS, K. P., HARDING, S. D., KATO, N., LEE, M. C. S., LUTH, M. R., MAZITSCHEK, R., MITTAL, N., NILES, J. C., OKOMBO, J., OTTILIE, S., PASAJE, C. F. A., PROBST, A. S., RAWAT, M., ROCAMORA, F., SAKATA-KATO, T., SOUTHAN, C., SPEDDING, M., TYE, M. A., YANG, T., ZHAO, N. & DAVIES, J. A. 2023. Advances in malaria pharmacology and the online guide to MALARIA PHARMACOLOGY: IUPHAR review 38. *Br J Pharmacol,* 180**,** 1899-1929.

ASANTE, K. P., ANSONG, D., KAALI, S., ADJEI, S., LIEVENS, M., NANA BADU, L., AGYAPONG DARKO, P., BOAKYE YIADOM BUABENG, P., BOAHEN, O., MARIA RETTIG, T., AGUTU, C., BENARD EKOW HARRISON, S., NTIAMOAH, Y., ADOMAKO ANIM, J., ADENIJI, E., AGORDO DORNUDO, A., GVOZDENOVIC, E., DOSOO, D., SAMBIAN, D., OWUSU-BOATENG, H., ATO WILSON, E., PREMPEH, F., VANDOOLAEGHE, P., SCHUERMAN, L., OWUSU-AGYEI, S., AGBENYEGA, T. & OFORI-ANYINAM, O. 2020. Immunogenicity and safety of the RTS,S/AS01 malaria vaccine co-administered with measles, rubella and yellow fever vaccines in Ghanaian children: A phase IIIb, multi-center, non-inferiority, randomized, open, controlled trial. *Vaccine,* 38**,** 3411-3421.

BANNISTER, L. & MITCHELL, G. 2003. The ins, outs and roundabouts of malaria. *Trends Parasitol,* 19**,** 209-13.

BARBER, B. E., FERNANDEZ, M., PATEL, H. B., BARCELO, C., WOOLLEY, S. D., PATEL, H., LLEWELLYN, S., ABD-RAHMAN, A. N., SHARMA, S., JAIN, M., GHOGHARI, A., DI RESTA, I., FUCHS, A., DENI, I., YEO, T., MOK, S., FIDOCK, D. A., CHALON, S., MOHRLE, J. J., PARMAR, D., MCCARTHY, J. S. & KANSAGRA, K. 2022. Safety, pharmacokinetics, and antimalarial activity of the novel triaminopyrimidine ZY-19489: a first-in-human, randomised, placebo-controlled, double-blind, single ascending dose study, pilot food-effect study, and volunteer infection study. *Lancet Infect Dis,* 22**,** 879-890.

BARTOLONI, A. & ZAMMARCHI, L. 2012. Clinical aspects of uncomplicated and severe malaria. *Mediterr J Hematol Infect Dis,* 4**,** e2012026.

BENELLI, G. & BEIER, J. C. 2017. Current vector control challenges in the fight against malaria. *Acta Trop,* 174**,** 91-96.

BHARTI, H., SINGAL, A., RAZA, M., GHOSH, P. C. & NAG, A. 2019. Ionophores as Potent Anti-malarials: A Miracle in the Making. *Curr Top Med Chem,* 18**,** 2029-2041.

BHATT, S., WEISS, D. J., CAMERON, E., BISANZIO, D., MAPPIN, B., DALRYMPLE, U., BATTLE, K., MOYES, C. L., HENRY, A., ECKHOFF, P. A., WENGER, E. A., BRIET, O., PENNY, M. A., SMITH, T. A., BENNETT, A., YUKICH, J., EISELE, T. P., GRIFFIN, J. T., FERGUS, C. A., LYNCH, M., LINDGREN, F., COHEN, J. M., MURRAY, C. L. J., SMITH, D. L., HAY, S. I., CIBULSKIS, R. E. & GETHING, P. W. 2015. The effect of malaria control on *Plasmodium falciparum* in Africa between 2000 and 2015. *Nature,* 526**,** 207-211.

BIRKHOLTZ, L., VAN BRUMMELEN, A. C., CLARK, K., NIEMAND, J., MARECHAL, E., LLINAS, M. & LOUW, A. I. 2008. Exploring functional genomics for drug target and therapeutics discovery in *Plasmodia*. *Acta Trop,* 105**,** 113-23.

BOYD, M. A., DAVIS, A. M., CHAMBERS, N. R., TRAN, P., PRINDLE, A. & KAMAT, N. P. 2021. Vesicle-Based Sensors for Extracellular Potassium Detection. *Cell Mol Bioeng,* 14**,** 459-469.

CAI, S., RISINGER, A. L., NAIR, S., PENG, J., ANDERSON, T. J., DU, L., POWELL, D. R., MOOBERRY, S. L. & CICHEWICZ, R. H. 2016. Identification of Compounds with Efficacy against Malaria Parasites from Common North American Plants. *J Nat Prod,* 79**,** 490-8.

CHAWLA, J., OBERSTALLER, J. & ADAMS, J. H. 2021. Targeting Gametocytes of the Malaria Parasite *Plasmodium falciparum* in a Functional Genomics Era: Next Steps. *Pathogens,* 10.

CHEUKA, P. M., CENTANI, L., ARENDSE, L. B., FIENBERG, S., WAMBUA, L., RENGA, S. S., DZIWORNU, G. A., KUMAR, M., LAWRENCE, N., TAYLOR, D., WITTLIN, S., COERTZEN, D., READER, J., VAN DER WATT, M., BIRKHOLTZ, L. M. & CHIBALE, K. 2021. New Amidated 3,6-Diphenylated Imidazopyridazines with Potent Antiplasmodium Activity Are Dual Inhibitors of *Plasmodium* Phosphatidylinositol-4-kinase and cGMP-Dependent Protein Kinase. *ACS Infect Dis,* 7**,** 34-46.

CHOI, L., MAJAMBERE, S. & WILSON, A. L. 2019. Larviciding to prevent malaria transmission. *Cochrane Database Syst Rev,* 8**,** CD012736.

CHRISTIE, R. M. 2011. Fluorescent dyes. *Handbook of textile and industrial dyeing.* Heriot -Watt University Woodhead publishing

COUNIHAN, N. A., MODAK, J. K. & DE KONING-WARD, T. F. 2021. How Malaria Parasites Acquire Nutrients From Their Host. *Front Cell Dev Biol,* 9**,** 649184.

CUI, L., MHARAKURWA, S., NDIAYE, D., RATHOD, P. K. & ROSENTHAL, P. J. 2015. Antimalarial Drug Resistance: Literature Review and Activities and Findings of the ICEMR Network. *Am J Trop Med Hyg,* 93**,** 57-68.

CUI, L. & SU, X. Z. 2009. Discovery, mechanisms of action and combination therapy of artemisinin. *Expert Rev Anti Infect Ther,* 7**,** 999-1013.

CYBULSKI, W., RADKO, L. & RZESKI, W. 2015. Cytotoxicity of monensin, narasin and salinomycin and their interaction with silybin in HepG2, LMH and L6 cell cultures. *Toxicol In Vitro,* 29**,** 337-44.

D'ALESSANDRO, S., CORBETT, Y., ILBOUDO, D. P., MISIANO, P., DAHIYA, N., ABAY, S. M., HABLUETZEL, A., GRANDE, R., GISMONDO, M. R., DECHERING, K. J., KOOLEN, K. M., SAUERWEIN, R. W., TARAMELLI, D., BASILICO, N. & PARAPINI, S. 2015. Salinomycin and other ionophores as a new class of antimalarial drugs with transmission-blocking activity. *Antimicrob Agents Chemother,* 59**,** 5135-44.

DAS, N. G., DHIMAN, S., TALUKDAR, P. K., GOSWAMI, D., RABHA, B., BARUAH, I. & VEER, V. 2015. Role of asymptomatic carriers and weather variables in persistent transmission of malaria in an endemic district of Assam, India. *Infect Ecol Epidemiol,* 5**,** 25442.

DAS, S., BHATANAGAR, S., MORRISEY, J. M., DALY, T. M., BURNS, J. M., JR., COPPENS, I. & VAIDYA, A. B. 2016. Na^+ Influx Induced by New Antimalarials Causes Rapid Alterations in the Cholesterol Content and Morphology of *Plasmodium falciparum*. *PLoS Pathog,* 12**,** e1005647.

DAVID, J. M. & RAJASEKARAN, A. K. 2015. Gramicidin A: A New Mission for an Old Antibiotic. *J Kidney Cancer VHL,* 2**,** 15-24.

DE CARVALHO, L. P., GROEGER-OTERO, S., KREIDENWEISS, A., KREMSNER, P. G., MORDMULLER, B. & HELD, J. 2021. Boromycin has Rapid-Onset Antibiotic Activity Against Asexual and Sexual Blood Stages of *Plasmodium falciparum*. *Front Cell Infect Microbiol,* 11**,** 802294.

DENNIS, A. S. M., LEHANE, A. M., RIDGWAY, M. C., HOLLERAN, J. P. & KIRK, K. 2018a. Cell Swelling Induced by the Antimalarial KAE609 (Cipargamin) and Other PfATP4-Associated Antimalarials. *Antimicrob Agents Chemother,* 62.

DENNIS, A. S. M., ROSLING, J. E. O., LEHANE, A. M. & KIRK, K. 2018b. Diverse antimalarials from whole-cell phenotypic screens disrupt malaria parasite ion and volume homeostasis. *Sci Rep,* 8**,** 8795.

DIXON, M. W. A. & TILLEY, L. 2021. *Plasmodium falciparum* goes bananas for sex. *Mol Biochem Parasitol,* 244**,** 111385.

EL-MOAMLY, A. A. & EL-SWEIFY, M. A. 2023. Malaria vaccines: the 60-year journey of hope and final success-lessons learned and future prospects. *Trop Med Health,* 51**,** 29.

ELLEKVIST, P., MACIEL, J., MLAMBO, G., RICKE, C. H., COLDING, H., KLAERKE, D. A. & KUMAR, N. 2008. Critical role of a K^+ channel in Plasmodium berghei transmission revealed by targeted gene disruption. *Proc Natl Acad Sci U S A,* 105**,** 6398-402.

ELLEKVIST, P., RICKE, C. H., LITMAN, T., SALANTI, A., COLDING, H., ZEUTHEN, T. & KLAERKE, D. A. 2004. Molecular cloning of a K^+ channel from the malaria parasite *Plasmodium falciparum*. *Biochem Biophys Res Commun,* 318**,** 477-84.

FANG, Y., SHI, W. Q., WU, J. T., LI, Y. Y., XUE, J. B. & ZHANG, Y. 2019. Resistance to pyrethroid and organophosphate insecticides, and the geographical distribution and polymorphisms of target-site

mutations in voltage-gated sodium channel and acetylcholinesterase 1 genes in Anopheles sinensis populations in Shanghai, China. *Parasit Vectors,* 12**,** 396.

GARCIA, G. E., WIRTZ, R. A., BARR, J. R., WOOLFITT, A. & ROSENBERG, R. 1998. Xanthurenic acid induces gametogenesis in *Plasmodium*, the malaria parasite. *J Biol Chem,* 273**,** 12003-5.

GARRIDO, A., LEPAILLEUR, A., MIGNANI, S. M., DALLEMAGNE, P. & ROCHAIS, C. 2020. hERG toxicity assessment: Useful guidelines for drug design. *Eur J Med Chem,* 195**,** 112290.

GATTON, M. L., MARTIN, L. B. & CHENG, Q. 2004. Evolution of resistance to sulfadoxine-pyrimethamine in *Plasmodium falciparum*. *Antimicrob Agents Chemother,* 48**,** 2116-23.

GENTON, B. 2023. R21/Matrix-M malaria vaccine: a new tool to achieve WHO's goal to eliminate malaria in 30 countries by 2030. *J Travel Med*.

GRASSO, F., FRATINI, F., ALBANESE, T. G., MOCHI, S., CIARDO, M., PACE, T., PONZI, M., PIZZI, E. & OLIVIERI, A. 2022. Identification and preliminary characterization of *Plasmodium falciparum* proteins secreted upon gamete formation. *Sci Rep,* 12**,** 9592.

GUMILA, C., ANCELIN, M. L., JEMINET, G., DELORT, A. M., MIQUEL, G. & VIAL, H. J. 1996. Differential *in vitro* activities of ionophore compounds against *Plasmodium falciparum* and mammalian cells. *Antimicrob Agents Chemother,* 40**,** 602-8.

HAMEED, P. S., SOLAPURE, S., PATIL, V., HENRICH, P. P., MAGISTRADO, P. A., BHARATH, S., MURUGAN, K., VISWANATH, P., PUTTUR, J., SRIVASTAVA, A., BELLALE, E., PANDUGA, V., SHANBAG, G., AWASTHY, D., LANDGE, S., MORAYYA, S., KOUSHIK, K., SARALAYA, R., RAICHURKAR, A., RAUTELA, N., ROY CHOUDHURY, N., AMBADY, A., NANDISHAIAH, R., REDDY, J., PRABHAKAR, K. R., MENASINAKAI, S., RUDRAPATNA, S., CHATTERJI, M., JIMENEZ-DIAZ, M. B., MARTINEZ, M. S., SANZ, L. M., COBURN-FLYNN, O., FIDOCK, D. A., LUKENS, A. K., WIRTH, D. F., BANDODKAR, B., MUKHERJEE, K., MCLAUGHLIN, R. E., WATERSON, D., ROSENBRIER-RIBEIRO, L., HICKLING, K., BALASUBRAMANIAN, V., WARNER, P., HOSAGRAHARA, V., DUDLEY, A., IYER, P. S., NARAYANAN, S., KAVANAGH, S. & SAMBANDAMURTHY, V. K. 2015. Triaminopyrimidine is a fast-killing and long-acting antimalarial clinical candidate. *Nat Commun,* 6**,** 6715.

HANBOONKUNUPAKARN, B., TARNING, J., PUKRITTAYAKAMEE, S. & CHOTIVANICH, K. 2022. Artemisinin resistance and malaria elimination: Where are we now? *Front Pharmacol,* 13**,** 876282.

HAYASHI, M., YAMADA, H., MITAMURA, T., HORII, T., YAMAMOTO, A. & MORIYAMA, Y. 2000. Vacuolar H^+-ATPase localized in plasma membranes of malaria parasite cells, *Plasmodium falciparum*, is involved in regional acidification of parasitized erythrocytes. *J Biol Chem,* 275**,** 34353-8.

IAMSHANOVA, O., MARIOT, P., LEHEN'KYI, V. & PREVARSKAYA, N. 2016. Comparison of fluorescence probes for intracellular sodium imaging in prostate cancer cell lines. *Eur Biophys J,* 45**,** 765-777.

IVERSEN, P. W., EASTWOOD, B. J., SITTAMPALAM, G. S. & COX, K. L. 2006. A comparison of assay performance measures in screening assays: signal window, Z' factor, and assay variability ratio. *J Biomol Screen,* 11**,** 247-52.

JOBSIS, P. D., ROTHSTEIN, E. C. & BALABAN, R. S. 2007. Limited utility of acetoxymethyl (AM)-based intracellular delivery systems, *in vivo*: interference by extracellular esterases. *J Microsc,* 226**,** 74-81.

KAISER, M. L., WOOD, O. R., DAMIENS, D., BROOKE, B. D., KOEKEMOER, L. L. & MUNHENGA, G. 2021. Estimates of the population size and dispersal range of *Anopheles arabiensis* in Northern KwaZulu-Natal, South Africa: implications for a planned pilot programme to release sterile male mosquitoes. *Parasit Vectors,* 14**,** 205.

KAVUNGA-MEMBO, H., ILOMBE, G., MASUMU, J., MATANGILA, J., IMPONGE, J., MANZAMBI, E., WASTENGA, F., NGOYI, D. M., VAN GEETRUYDEN, J. P. & MUYEMBE, J. J. 2018. Molecular identification of *Plasmodium* species in symptomatic children of Democratic Republic of Congo. *Malar J,* 17**,** 334.

KHAMMY, M. M., KIM, S., BENTZEN, B. H., LEE, S., CHOI, I., AALKJAER, C. & JEPPS, T. A. 2018. 4-Aminopyridine: a pan voltage-gated potassium channel inhibitor that enhances K(v) 7.4 currents and inhibits noradrenaline-mediated contraction of rat mesenteric small arteries. *Br J Pharmacol,* 175**,** 501-516.

KILLEEN, G. F., MASALU, J. P., CHINULA, D., FOTAKIS, E. A., KAVISHE, D. R., MALONE, D. & OKUMU, F. 2017. Control of Malaria Vector Mosquitoes by Insecticide-Treated Combinations of Window Screens and Eave Baffles. *Emerg Infect Dis,* 23**,** 782-789.

KIRK, K. 2015. Ion Regulation in the Malaria Parasite. *Annu Rev Microbiol,* 69**,** 341-59.

KRISHNA, S., WOODROW, C., WEBB, R., PENNY, J., TAKEYASU, K., KIMURA, M. & EAST, J. M. 2001. Expression and functional characterization of a *Plasmodium falciparum* Ca^{2+}-ATPase (PfATP4) belonging to a subclass unique to apicomplexan organisms. *J Biol Chem,* 276**,** 10782-7.

LALREMRUATA, A., JEYARAJ, S., ENGLEITNER, T., JOANNY, F., LANG, A., BELARD, S., MOMBO-NGOMA, G., RAMHARTER, M., KREMSNER, P. G., MORDMULLER, B. & HELD, J. 2017. Species and genotype diversity of *Plasmodium* in malaria patients from Gabon analysed by next generation sequencing. *Malar J,* 16**,** 398.

LAMBROS, C. & VANDERBERG, J. P. 1979. Synchronization of *Plasmodium falciparum* erythrocytic stages in culture. *J Parasitol,* 65**,** 418-20.

LANGRETH, S. G., JENSEN, J. B., REESE, R. T. & TRAGER, W. 1978. Fine structure of human malaria *in vitro*. *J Protozool,* 25**,** 443-52.

LAURENS, M. B. 2020. RTS,S/AS01 vaccine (Mosquirix): an overview. *Hum Vaccin Immunother,* 16**,** 480-489.

LEE, P., YE, Z., VAN DYKE, K. & KIRK, R. G. 1988. X-ray microanalysis of *Plasmodium falciparum* and infected red blood cells: effects of qinghaosu and chloroquine on potassium, sodium, and phosphorus composition. *Am J Trop Med Hyg,* 39**,** 157-65.

LEHANE, A. M., RIDGWAY, M. C., BAKER, E. & KIRK, K. 2014. Diverse chemotypes disrupt ion homeostasis in the Malaria parasite. *Mol Microbiol,* 94**,** 327-39.

LIM, H. H., SHANE, T. & MILLER, C. 2012. Intracellular proton access in a Cl^-/H^+ antiporter. *PLoS Biol,* 10**,** e1001441.

MAARTENS, G. 2008. Severe malaria. *CME : Your SA Journal of CPD,* 26**,** 294-295.

MADDISON, P. & NEWSOM-DAVIS, J. 2003. Treatment for Lambert-Eaton myasthenic syndrome. *Cochrane Database Syst Rev***,** CD003279.

MAHER, M. P., WU, N. T. & AO, H. 2007. pH-Insensitive FRET voltage dyes. *J Biomol Screen,* 12**,** 656-67.

MAHTAL, N., WU, Y., CINTRAT, J. C., BARBIER, J., LEMICHEZ, E. & GILLET, D. 2020. Revisiting Old Ionophore Lasalocid as a Novel Inhibitor of Multiple Toxins. *Toxins (Basel),* 12.

MARTIN, R. E. 2020. The transportome of the malaria parasite. *Biol Rev Camb Philos Soc,* 95**,** 305-332.

MAURITZ, J. M., SEEAR, R., ESPOSITO, A., KAMINSKI, C. F., SKEPPER, J. N., WARLEY, A., LEW, V. L. & TIFFERT, T. 2011. X-ray microanalysis investigation of the changes in Na^+, K^+, and hemoglobin concentration in *Plasmodium falciparum*-infected red blood cells. *Biophys J,* 100**,** 1438-45.

MESSINA, V., VALTIERI, M., RUBIO, M., FALCHI, M., MANCINI, F., MAYOR, A., ALANO, P. & SILVESTRINI, F. 2018. Gametocytes of the Malaria Parasite *Plasmodium falciparum* Interact With and Stimulate Bone Marrow Mesenchymal Cells to Secrete Angiogenetic Factors. *Front Cell Infect Microbiol,* 8**,** 50.

MEUWIS, K., BOENS, N., DE SCHRYVER, F. C., GALLAY, J. & VINCENT, M. 1995. Photophysics of the fluorescent K^+ indicator PBFI. *Biophys J,* 68**,** 2469-73.

MINTA, A. & TSIEN, R. Y. 1989. Fluorescent indicators for cytosolic sodium. *J Biol Chem,* 264**,** 19449-57.

MOERSDORF, D., EGEE, S., HAHN, C., HANF, B., ELLORY, C., THOMAS, S. & BERNHARDT, I. 2013. Transmembrane potential of red blood cells under low ionic strength conditions. *Cell Physiol Biochem,* 31**,** 875-82.

MOON, S., LEE, S., KIM, H., FREITAS-JUNIOR, L. H., KANG, M., AYONG, L. & HANSEN, M. A. 2013. An image analysis algorithm for malaria parasite stage classification and viability quantification. *PLoS One,* 8**,** e61812.

MORGAN, A. J. & JACOB, R. 1994. Ionomycin enhances Ca^{2+} influx by stimulating store-regulated cation entry and not by a direct action at the plasma membrane. *Biochem J,* 300 (Pt 3)**,** 665-72.

MPOFU, M., BECKER, P., MUDAMBO, K. & DE JAGER, C. 2016. Field effectiveness of microbial larvicides on mosquito larvae in malaria areas of Botswana and Zimbabwe. *Malar J,* 15**,** 586.

NAGANO, T. 2010. Development of fluorescent probes for bioimaging applications. *Proc Jpn Acad Ser B Phys Biol Sci,* 86**,** 837-47.

NANA, R. R. D., HAWADAK, J., FOKO, L. P. K., KUMAR, A., CHAUDHRY, S., ARYA, A. & SINGH, V. 2023. Intermittent preventive treatment with Sulfadoxine pyrimethamine for malaria: a global overview and challenges affecting optimal drug uptake in pregnant women. *Pathog Glob Health,* 117**,** 462-475.

NICOLETTI, M. 2020. *Insect-borne diseases in the 21st century,* London, United Kingdom ; San Diego, CA, Academic Press.

NIEMAND, J., VAN BILJON, R., VAN DER WATT, M., VAN HEERDEN, A., READER, J., VAN WYK, R., ORCHARD, L., CHIBALE, K., LLINAS, M. & BIRKHOLTZ, L. M. 2021. Chemogenomic Fingerprints Associated with Stage-Specific Gametocytocidal Compound Action against Human Malaria Parasites. *ACS Infect Dis,* 7**,** 2904-2916.

OLIVEIRA, E., BERTOLO, E., NUNEZ, C., PILLA, V., SANTOS, H. M., FERNANDEZ-LODEIRO, J., FERNANDEZ-LODEIRO, A., DJAFARI, J., CAPELO, J. L. & LODEIRO, C. 2018. Green and Red Fluorescent Dyes for Translational Applications in Imaging and Sensing Analytes: A Dual-Color Flag. *ChemistryOpen,* 7**,** 3.

OTOGURO, K., KOHANA, A., MANABE, C., ISHIYAMA, A., UI, H., SHIOMI, K., YAMADA, H. & OMURA, S. 2001. Potent antimalarial activities of polyether antibiotic, X-206. *J Antibiot (Tokyo),* 54**,** 658-63.

OTTEN-KUIPERS, M. A., ROELOFSEN, B. & OP DEN KAMP, J. A. 1995. Stage-dependent effects of analogs of gramicidin A on the growth of *Plasmodium falciparum in vitro*. *Parasitol Res,* 81**,** 26-31.

OVERMAN, R. R. 1948. Reversible cellular permeability alterations in disease; *in vivo* studies on sodium, potassium and chloride concentrations in erythrocytes of the malarious monkey. *Am J Physiol,* 152**,** 113-21.

PILLAI, A. D., ADDO, R., SHARMA, P., NGUITRAGOOL, W., SRINIVASAN, P. & DESAI, S. A. 2013. Malaria parasites tolerate a broad range of ionic environments and do not require host cation remodelling. *Mol Microbiol,* 88**,** 20-34.

PLOUFFE, D., BRINKER, A., MCNAMARA, C., HENSON, K., KATO, N., KUHEN, K., NAGLE, A., ADRIAN, F., MATZEN, J. T., ANDERSON, P., NAM, T. G., GRAY, N. S., CHATTERJEE, A., JANES, J., YAN, S. F., TRAGER, R., CALDWELL, J. S., SCHULTZ, P. G., ZHOU, Y. & WINZELER, E. A. 2008. *In silico* activity profiling reveals the mechanism of action of antimalarials discovered in a high-throughput screen. *Proc Natl Acad Sci U S A,* 105**,** 9059-64.

PRESSMAN, B. C. 1968. Ionophorous antibiotics as models for biological transport. *Fed Proc,* 27**,** 1283-8.

PRIEST, B. T., BELL, I. M. & GARCIA, M. L. 2008. Role of hERG potassium channel assays in drug development. *Channels (Austin),* 2**,** 87-93.

RADOSINSKA, J. & VRBJAR, N. 2016. The role of red blood cell deformability and Na^+,K^+-ATPase function in selected risk factors of cardiovascular diseases in humans: focus on hypertension, diabetes mellitus and hypercholesterolemia. *Physiol Res,* 65 Suppl 1**,** S43-54.

RANA, P. S., GIBBONS, B. A., VERENINOV, A. A., YURINSKAYA, V. E., CLEMENTS, R. J., MODEL, T. A. & MODEL, M. A. 2019. Calibration and characterization of intracellular Asante Potassium Green probes, APG-2 and APG-4. *Anal Biochem,* 567**,** 8-13.

RAZA, M., BHARTI, H., SINGAL, A., NAG, A. & GHOSH, P. C. 2018. Long circulatory liposomal maduramicin inhibits the growth of *Plasmodium falciparum* blood stages in culture and cures murine models of experimental malaria. *Nanoscale,* 10**,** 13773-13791.

READER, J., VAN DER WATT, M. E., TAYLOR, D., LE MANACH, C., MITTAL, N., OTTILIE, S., THERON, A., MOYO, P., ERLANK, E., NARDINI, L., VENTER, N., LAUTERBACH, S., BEZUIDENHOUT, B., HORATSCHECK, A., VAN HEERDEN, A., SPILLMAN, N. J., COWELL, A. N., CONNACHER, J., OPPERMAN, D., ORCHARD, L. M., LLINAS, M., ISTVAN, E. S., GOLDBERG, D. E., BOYLE, G. A., CALVO, D., MANCAMA, D., COETZER, T. L., WINZELER, E. A., DUFFY, J., KOEKEMOER, L. L., BASARAB, G., CHIBALE, K. & BIRKHOLTZ, L. M. 2021. Multistage and transmission-blocking targeted antimalarials discovered from the open-source MMV Pandemic Response Box. *Nat Commun,* 12**,** 269.

REED, P. W. & LARDY, H. A. 1972. A23187: a divalent cation ionophore. *J Biol Chem,* 247**,** 6970-7.

RICHIE, T. L. & SAUL, A. 2002. Progress and challenges for malaria vaccines. *Nature,* 415**,** 694-701.

RIMMELE, T. S. & CHATTON, J. Y. 2014. A novel optical intracellular imaging approach for potassium dynamics in astrocytes. *PLoS One,* 9**,** e109243.

ROSSATI, A., BARGIACCHI, O., KROUMOVA, V., ZARAMELLA, M., CAPUTO, A. & GARAVELLI, P. L. 2016. Climate, environment and transmission of malaria. *Infez Med,* 24**,** 93-104.

ROTTMANN, M., MCNAMARA, C., YEUNG, B. K., LEE, M. C., ZOU, B., RUSSELL, B., SEITZ, P., PLOUFFE, D. M., DHARIA, N. V., TAN, J., COHEN, S. B., SPENCER, K. R., GONZALEZ-PAEZ, G. E., LAKSHMINARAYANA, S. B., GOH, A., SUWANARUSK, R., JEGLA, T., SCHMITT, E. K., BECK, H. P., BRUN, R., NOSTEN, F., RENIA, L., DARTOIS, V., KELLER, T. H., FIDOCK, D. A., WINZELER, E. A. & DIAGANA, T. T. 2010. Spiroindolones, a potent compound class for the treatment of malaria. *Science,* 329**,** 1175-80.

SALIBA, K. J., HORNER, H. A. & KIRK, K. 1998. Transport and metabolism of the essential vitamin pantothenic acid in human erythrocytes infected with the malaria parasite *Plasmodium falciparum*. *J Biol Chem,* 273**,** 10190-5.

SALIBA, K. J. & KIRK, K. 1999. pH regulation in the intracellular malaria parasite, *Plasmodium falciparum*. H^+ extrusion via a V-type H^+-ATPase. *J Biol Chem,* 274**,** 33213-9.

SCHMITT, E. K., NDAYISABA, G., YEKA, A., ASANTE, K. P., GROBUSCH, M. P., KARITA, E., MUGERWA, H., ASIIMWE, S., ODURO, A., FOFANA, B., DOUMBIA, S., SU, G., CSERMAK RENNER, K., VENISHETTY, V. K., SAYYED, S., STRAIMER, J., DEMIN, I., BARSAINYA, S., BOULTON, C. & GANDHI, P. 2022. Efficacy of Cipargamin (KAE609) in a Randomized, Phase II Dose-Escalation Study in Adults in Sub-Saharan Africa With Uncomplicated *Plasmodium falciparum* Malaria. *Clin Infect Dis,* 74**,** 1831-1839.

SOULARD, V., BOSSON-VANGA, H., LORTHIOIS, A., ROUCHER, C., FRANETICH, J. F., ZANGHI, G., BORDESSOULLES, M., TEFIT, M., THELLIER, M., MOROSAN, S., LE NAOUR, G., CAPRON, F., SUEMIZU, H., SNOUNOU, G., MORENO-SABATER, A. & MAZIER, D. 2015. *Plasmodium falciparum* full life cycle and *Plasmodium ovale* liver stages in humanized mice. *Nat Commun,* 6**,** 7690.

SPIELMANN, T. & BECK, H. P. 2000. Analysis of stage-specific transcription in *Plasmodium falciparum* reveals a set of genes exclusively transcribed in ring stage parasites. *Mol Biochem Parasitol,* 111**,** 453-8.

SPILLMAN, N. J., ALLEN, R. J. & KIRK, K. 2013a. Na^+ extrusion imposes an acid load on the intraerythrocytic malaria parasite. *Mol Biochem Parasitol,* 189**,** 1-4.

SPILLMAN, N. J., ALLEN, R. J., MCNAMARA, C. W., YEUNG, B. K., WINZELER, E. A., DIAGANA, T. T. & KIRK, K. 2013b. Na^+ regulation in the malaria parasite *Plasmodium falciparum* involves the cation ATPase PfATP4 and is a target of the spiroindolone antimalarials. *Cell Host Microbe,* 13**,** 227-37.

SPILLMAN, N. J. & KIRK, K. 2015. The malaria parasite cation ATPase PfATP4 and its role in the mechanism of action of a new arsenal of antimalarial drugs. *Int J Parasitol Drugs Drug Resist,* 5**,** 149-62.

STURM, A., AMINO, R., VAN DE SAND, C., REGEN, T., RETZLAFF, S., RENNENBERG, A., KRUEGER, A., POLLOK, J. M., MENARD, R. & HEUSSLER, V. T. 2006. Manipulation of host hepatocytes by the malaria parasite for delivery into liver sinusoids. *Science,* 313**,** 1287-90.

SWART, T., KHAN, F. D., NTLANTSANA, A., LAMING, D., VEALE, C. G. L., PRZYBORSKI, J. M., EDKINS, A. L. & HOPPE, H. C. 2020. Detection of the *in vitro* modulation of *Plasmodium falciparum* Arf1 by Sec7 and ArfGAP domains using a colorimetric plate-based assay. *Sci Rep,* 10**,** 4193.

TALMAN, A. M., DOMARLE, O., MCKENZIE, F. E., ARIEY, F. & ROBERT, V. 2004. Gametocytogenesis: the puberty of *Plasmodium falciparum*. *Malar J,* 3**,** 24.

TRAGER, W. & JENSEN, J. B. 1976. Human malaria parasites in continuous culture. *Science,* 193**,** 673-5.

TRAMPUZ, A., JEREB, M., MUZLOVIC, I. & PRABHU, R. M. 2003. Clinical review: Severe malaria. *Crit Care,* 7**,** 315-23.

VAN DER WATT, M. E., READER, J., CHURCHYARD, A., NONDABA, S. H., LAUTERBACH, S. B., NIEMAND, J., ABAYOMI, S., VAN BILJON, R. A., CONNACHER, J. I., VAN WYK, R. D. J., LE MANACH, C., PAQUET, T., GONZALEZ CABRERA, D., BRUNSCHWIG, C., THERON, A., LOZANO-ARIAS, S., RODRIGUES, J. F. I., HERREROS, E., LEROY, D., DUFFY, J., STREET, L. J., CHIBALE, K., MANCAMA, D., COETZER, T. L. & BIRKHOLTZ, L. M. 2018. Potent *Plasmodium falciparum* gametocytocidal compounds identified by exploring the kinase inhibitor chemical space for dual active antimalarials. *J Antimicrob Chemother,* 73**,** 1279-1290.

VAN SCHALKWYK, D. A., CHAN, X. W., MISIANO, P., GAGLIARDI, S., FARINA, C. & SALIBA, K. J. 2010. Inhibition of *Plasmodium falciparum* pH regulation by small molecule indole derivatives results in rapid parasite death. *Biochem Pharmacol,* 79**,** 1291-9.

VAN VOORHIS, W. C., ADAMS, J. H., ADELFIO, R., AHYONG, V., AKABAS, M. H., ALANO, P., ALDAY, A., ALEMAN RESTO, Y., ALSIBAEE, A., ALZUALDE, A., ANDREWS, K. T., AVERY, S. V., AVERY, V. M., AYONG, L., BAKER, M., BAKER, S., BEN MAMOUN, C., BHATIA, S., BICKLE, Q., BOUNAADJA, L., BOWLING, T., BOSCH, J., BOUCHER, L. E., BOYOM, F. F., BREA, J., BRENNAN, M., BURTON, A., CAFFREY, C. R., CAMARDA, G., CARRASQUILLA, M., CARTER, D., BELEN CASSERA, M., CHIH-CHIEN CHENG, K., CHINDAUDOMSATE, W., CHUBB, A., COLON, B. L., COLON-LOPEZ, D. D., CORBETT, Y., CROWTHER, G. J., COWAN, N., D'ALESSANDRO, S., LE DANG, N., DELVES, M., DERISI, J. L., DU, A. Y., DUFFY, S., ABD EL-SALAM EL-SAYED, S., FERDIG, M. T., FERNANDEZ ROBLEDO, J. A., FIDOCK, D. A., FLORENT, I., FOKOU, P. V., GALSTIAN, A., GAMO, F. J., GOKOOL, S., GOLD, B., GOLUB, T., GOLDGOF, G. M., GUHA, R., GUIGUEMDE, W. A., GURAL, N., GUY, R. K., HANSEN, M. A., HANSON, K. K., HEMPHILL, A., HOOFT VAN HUIJSDUIJNEN, R., HORII, T., HORROCKS, P., HUGHES, T. B., HUSTON, C., IGARASHI, I., INGRAM-SIEBER, K., ITOE, M. A., JADHAV, A., NARANUNTARAT JENSEN, A., JENSEN, L. T., JIANG, R. H., KAISER, A., KEISER, J., KETAS, T., KICKA, S., KIM, S., KIRK, K., KUMAR, V. P., KYLE, D. E., LAFUENTE, M. J., LANDFEAR, S., LEE, N., LEE, S., LEHANE, A. M., LI, F., LITTLE, D., LIU, L., LLINAS, M., LOZA, M. I., LUBAR, A., LUCANTONI, L., LUCET, I., MAES, L., MANCAMA, D., et al. 2016. Open Source Drug Discovery with the Malaria Box Compound Collection for Neglected Diseases and Beyond. *PLoS Pathog,* 12**,** e1005763.

VAN ZYL, R. L. 2018. Prophylaxis - A key component in malaria control. *South African Family Practice*.

VENUGOPAL, K., HENTZSCHEL, F., VALKIUNAS, G. & MARTI, M. 2020. *Plasmodium* asexual growth and sexual development in the haematopoietic niche of the host. *Nat Rev Microbiol,* 18**,** 177-189.

WALLER, K. L., KIM, K. & MCDONALD, T. V. 2008a. *Plasmodium falciparum*: growth response to potassium channel blocking compounds. *Exp Parasitol,* 120**,** 280-5.

WALLER, K. L., MCBRIDE, S. M., KIM, K. & MCDONALD, T. V. 2008b. Characterization of two putative potassium channels in *Plasmodium falciparum*. *Malar J,* 7**,** 19.

WHITE, N. J. 2017. Malaria parasite clearance. *Malar J,* 16**,** 88.

WINTERBERG, M. & KIRK, K. 2016. A high-sensitivity HPLC assay for measuring intracellular Na^+ and K^+ and its application to *Plasmodium falciparum* infected erythrocytes. *Sci Rep,* 6**,** 29241.

WORLD HEALTH ORGANIZATION 2017. Intermittent preventive treatment of malaria in pregnancy (IPTp) Geneva: World Health Organization.

WORLD HEALTH ORGANIZATION 2023. World malaria report

XU, M., HU, Y. X., LU, S. N., IDRIS, M. A., ZHOU, S. D., YANG, J., FENG, X. N., HUANG, Y. M., XU, X., CHEN, Y. & WANG, D. Q. 2023. Seasonal malaria chemoprevention in Africa and China's upgraded role as a contributor: a scoping review. *Infect Dis Poverty,* 12**,** 63.

YAMADA, A., GAJA, N., OHYA, S., MURAKI, K., NARITA, H., OHWADA, T. & IMAIZUMI, Y. 2001. Usefulness and limitation of $DiBAC_4(3)$, a voltage-sensitive fluorescent dye, for the measurement of membrane potentials regulated by recombinant large conductance Ca^{2+}-activated K^+ channels in HEK293 cells. *Jpn J Pharmacol,* 86**,** 342-50.

YANG, T., OTTILIE, S., ISTVAN, E. S., GODINEZ-MACIAS, K. P., LUKENS, A. K., BARAGANA, B., CAMPO, B., WALPOLE, C., NILES, J. C., CHIBALE, K., DECHERING, K. J., LLINAS, M., LEE, M. C. S., KATO, N., WYLLIE, S., MCNAMARA, C. W., GAMO, F. J., BURROWS, J., FIDOCK, D. A., GOLDBERG, D. E., GILBERT, I. H., WIRTH, D. F., WINZELER, E. A. & MALARIA DRUG ACCELERATOR, C. 2021. MalDA, Accelerating Malaria Drug Discovery. *Trends Parasitol,* 37**,** 493-507.

YOON, S. A., PARK, S. Y., CHA, Y., GOPALA, L. & LEE, M. H. 2021. Strategies of Detecting Bacteria Using Fluorescence-Based Dyes. *Front Chem,* 9**,** 743923.

ZHANG, J. H., CHUNG, T. D. & OLDENBURG, K. R. 1999. A Simple Statistical Parameter for Use in Evaluation and Validation of High Throughput Screening Assays. *J Biomol Screen,* 4**,** 67-73.

ZHOU, Y., XIA, X. M. & LINGLE, C. J. 2020. The functionally relevant site for paxilline inhibition of BK channels. *Proc Natl Acad Sci U S A,* 117**,** 1021-1026.

ZHU, H., FAN, J., DU, J. & PENG, X. 2016. Fluorescent Probes for Sensing and Imaging within Specific Cellular Organelles. *Acc Chem Res,* 49**,** 2115-2126.